

AN EXPERIMENTAL STUDY ON THE TRIBOLOGICAL EFFECTS OF  
TARGETTED CUTTING FLUID COMBINATIONS ON SURFACE  
INTEGRITY OF MACHINED AISI 1045 STEEL

by

Himabindu Nunna

A thesis submitted to the faculty of  
The University of Utah  
in partial fulfillment of the requirements for the degree of

Master of Science

Department of Mechanical Engineering

The University of Utah

August 2012

Copyright © Himabindu Nunna 2012

All Rights Reserved



## **ABSTRACT**

In order to enable sustainable manufacturing, the indiscriminate use of cutting fluids in modern machining has to be tackled, given its environmental and economic impacts. A possible solution is the recent entrance of dry and near dry minimal quantity cooling and lubrication (MQC/L) machining. In order to evaluate the effectiveness and performance of MQC/L, however, further studies need to be done. The three major functions of cutting fluids are to perform cooling, lubrication, and chip removal from the cutting zone. The main objective of this work is to understand how the tribological aspects (cutting forces, chip flow, tool-chip contact area), chip morphology, and surface roughness and surface integrity (residual stresses) are influenced by i) the application of different cutting fluid combinations in minimal quantities ii) the direction of application of the cutting fluid in the facing of AISI 1045 steel using an uncoated flat-faced carbide tool.

A Minimal Quantity Cutting Fluid (MQCF) dispensing system was tested and implemented to evaluate the effects of differing fluid dispensing rates and target directions. It was found that the effects of targeted cutting fluid combinations on the tribological aspects were significant when compared to dry machining, although the variation in the tribological aspects was marginal amongst the different cutting fluid combinations. In contrast, directing the coolant on the flank face of the tool revealed some interesting results. Compressive residual stresses were observed when coolant was

directed to the tool flank face as opposed to other cases, which generated tensile residual stresses in the machined subsurface. This suggests that localized and carefully chosen cutting fluid target direction and combination can enhance product performance by enhancing machining performance and surface integrity.

In summary, this thesis presents the significance of targeted minimal cutting fluid application in relation to machining performance (especially surface integrity) under the given cutting conditions and provides several recommendations for future work.

## TABLE OF CONTENTS

ABSTRACT.....	iii
LIST OF TABLES.....	vii
LIST OF FIGURES.....	viii
Chapters	
1. INTRODUCTION.....	1
1.1 Importance of Cutting Fluid in Machining.....	2
1.2 Residual Stress Effects.....	5
1.3 Thesis Overview.....	7
1.4 References.....	9
2. BACKGROUND.....	10
2.1 Minimum Quantity Cooling and Lubrication.....	10
2.2 Chip Morphology.....	13
2.3 Surface Roughness.....	14
2.4 Residual Stresses.....	15
2.5 References.....	18
3. EXPERIMENTAL PLAN AND SETUP.....	22
3.1 Experimental Plan.....	22
3.2 Minimum Quantity Cutting Fluid Dispensing System.....	26
3.3 Measurement of Tribological Parameters.....	29
3.3.1 Prediction of Chip Flow Angle.....	29
3.3.2 Tool-Chip Contact Area.....	29
3.3.3 Chip Morphology.....	30
3.3.4 Surface Roughness.....	30
3.4 Residual Stress Measurement.....	30
3.4.1 Hole Drilling and Strains Acquisition.....	31
3.4.2 Residual Stress Calculation.....	33

3.5	References.....	35
4.	RESULTS AND DISCUSSION.....	37
4.1	Machining Forces.....	38
4.2	Prediction of Chip flow Angle.....	39
4.3	Tool-Chip Contact and Chip Morphology.....	41
4.4	Surface Roughness.....	45
4.5	Residual Stresses.....	46
4.6	Discussion.....	55
4.2	References.....	57
5.	SUMMARY AND SCOPE FOR FUTURE WORK.....	59

## LIST OF TABLES

3.1	Chemical composition of AISI 1045 steel.....	23
3.2	Cutting fluid combinations.....	25
4.1	Cutting fluid combinations.....	38



## LIST OF FIGURES

1.1	Ploughing phenomenon.....	6
3.1	Experimental setup.....	25
3.2	Flowchart of the Minimum Quantity Cutting Fluid (MQCF) dispensing system	26
3.4	Strain-gage rosette, directions.....	32
4.1	Force data.....	40
4.2	Chip flow angle.....	40
4.3	Tool-chip contact area.....	42
4.4	Tool chip interfacial contact.....	43
4.5	Chip forms obtained at different cutting fluid combinations.....	44
4.6	Surface roughness.....	46
4.7	Residual stress plot-Dry Vs 100% lubricant on the rake face.....	48
4.8	Residual stress plot-Dry Vs 25% coolant and 75% lubricant on the rake face.....	49
4.9	Residual stress plot-Dry Vs 50% coolant and 50% lubricant on the rake face.....	50
4.10	Residual stress plot-Dry Vs 75% coolant and 25% lubricant on the rake face.....	50
4.11	Residual stress plot-Dry Vs 100% coolant on the rake face.....	51

4.12 Residual stress plot–Dry Vs 100% coolant on the tool flank face.....	51
4.13 Peak residual stresses.....	54

## **CHAPTER 1**

### **INTRODUCTION**

The role of manufacturing in global industrialization is inevitable. Over the years, advanced technologies have provided tremendous growth in manufacturing processes. Developments in the latest technologies, labor and environmental laws, and industrial competitiveness have assigned rigorous stipulations on economics of manufacturing. Sustainable practices through energy saving, environment, and worker safety play a vital role when there is a demand for increased productivity.

In metal manufacturing processes, cutting fluid costs tend to be 7-17% of the total manufacturing costs, while the cutting tool costs account for 2-4% [6]. The alternatives are to use dry cutting or near zero lubrication/cooling in a compressed air jet that involves a minimal amount of lubricant or coolant or both as opposed to conventional cutting fluid amounts delivered in a continuous flood. This can affect production cost, worker health, environment, and waste disposal in a positive manner.

This work presents a study on the effects of application of controlled amounts of cutting fluids on tribological effects and surface integrity in machined surfaces. A specific focus of this thesis is understanding the impact of the location at which the lubricant/coolant is disposed on the tool surfaces. Correspondingly, the development of

the Minimum Quantity Cutting Fluid Dispensing System [3] used for the tests is also described in the following chapters.

Machining experiments were conducted on AISI 1045 steel bars using an uncoated carbide tool under different cutting fluid environments as well as with dry machining. A medium-carbon steel with 0.43% carbon with adequate strength and toughness is valuable for induction-hardened or flame-hardened components. Various industrial applications of 1045 steel are shafts, cams, pins, axles, rods, studs, machine parts, bolts, gears, pinions, forgings, bulldozer edges, ball bearings, F clamps, couplers, plungers, levers, and worm wheels [1,7]. This wide range of application is because of its advantage of hardness and higher wear and load resistance. AISI 1045 steel is also a well-modeled material in the literature, albeit with minimal knowledge on the effects of cutting fluid application on its machining characteristics.

In this thesis, the specific parameters studied in detail through the experimental study were cutting forces, surface integrity (as exemplified by surface and subsurface residual stresses), surface roughness, and chip flow direction and tool chip contact area (which characterizes the tribological effects).

### 1.1 Importance of Cutting Fluid in Machining

Conventional machining involves removal of material through a mechanical shearing action in the form of chips using cutting tools (harder than the material) to produce a desired shape and surface as the output. During the process, the contact among work piece-tool-chip can cause plastic deformation and temperature rise at the work zone, which in turn leads to increase in strain rates on the surface of the work piece and

localized phase transformations at the work piece-tool-chip interfaces, respectively [9,10].

The quality/efficiency of the finished work piece is measured by analyzing various parameters such as surface roughness, dimensional accuracy, subsurface microstructure, and residual stress distribution. Associated factors such as cutting forces (indicative of the power needed to cut the material) and tool-wear and tool-life (which have strong quality impacts on machined surfaces as well as impacts through reduced productivity and increased costs) are also important parameters. Cutting fluids come into the picture when the above-mentioned parameters are to be regulated. Lubrication, cooling, and chip transportation away from the cutting zone are the major functions of cutting fluids. There are four basic types of cutting fluids [5]:

1. Straight oil fluids: These nonemulsifiable fluids are used in an undiluted form for relatively low cutting speed operations such as gear hobbing and broaching. They are composed of a base mineral or petroleum oil and often contain polar lubricants like esters, fats, and vegetable oils as well as extreme pressure additives that include Chlorine, Phosphorus, and Sulphur. These fluids provide the best lubrication and poorest cooling characteristics compared to other types.
2. Soluble oil fluids: These fluids form an emulsion when mixed with water along with some emulsifying agents. The base mineral oil (30-85% oil) is diluted to 3-20% concentrate by volume that provides good lubrication and heat transfer performance. They are least the expensive and widely used in industry among all cutting fluids.

3. Synthetic fluids: These fluids are formulated from alkaline inorganic and organic compounds along with additives for corrosion inhibition and they do not contain a petroleum or mineral oil base. They are usually diluted with water at 3 to 10% of the concentrate and provide the best cooling performance of all cutting fluids, but very little lubrication.
4. Semisynthetic fluids: These fluids are a combination of synthetic and soluble oil fluids and they combine the lubricating and cooling characteristics of both types. They are diluted to contain 5-30% of the concentrate. Semisynthetic fluids fall between soluble oil fluids and synthetic fluids in terms of cost and heat transfer performance.

Cutting fluids are mixed with air jets under pressure and dispensed on the cutting zone through external nozzles. They can also be dispensed internally through the tool-tip (typically in drills). The alternate method to conventional flooding is minimum quantity cooling/lubrication with mist/spray application. This minimum quantity lubrication/cooling machining (near-dry machining) has various effects on different aspects, such as:

- Cutting fluid replaces completely dry machining, leading to a better tool life and reducing the amount of fluid injected as opposed to flood machining

- Cutting fluid helps in reducing tool-chip contact length and hence reduces temperature rise and friction at the tool-chip interface

- The chips from the cutting zone can be cleared away by the cutting fluid flow under compressed air jet

-The waste disposal of the cutting fluids is expected to be minimal when compared to flood cooling.

## 1.2 Residual Stress Effects

Residual stresses are stresses that remain in a solid body after the removal of external loading that include mechanical and thermal loads. During a machining process, residual stresses can be formed due to various inhomogeneous material deformation, such as mechanical loading, thermal gradient, and phase transformation [2,8].

Residual stress serves as a key factor in significantly influencing the final product performance such as fatigue life, creep, corrosion, wear, and dimensional accuracy of a machined component.

Depending upon its magnitude, pattern, and distribution, residual stress may be either beneficial or detrimental, either of which can be recognized only when a failure occurs. Compressive residual stresses are usually beneficial to fatigue life, creep life, and resistance to stress corrosion cracking, while tensile residual stresses are detrimental to the same properties mentioned.

Residual stresses are generally classified into two types based on range or distance over which they can be observed. The macro residual stresses exist in the order of hundreds of microns while the micro residual stresses cover a distance of a few grains or a part of a grain.

During chip formation, a part of the material is pushed upward by the rake face while the part below the uncut chip thickness is ploughed under the cutting edge, experiencing high transient stresses, large strains, and strain-rates at high temperatures with severe

gradients. Hence, this thin ploughed layer chiefly contributes as a factor to residual stress as opposed to the chip flowing away [4]. Figure 1.1 shows the ploughing phenomenon that was explained in the predictive model and validation of unique hook-shaped residual stress profiles in hard turning.

Since most modern cutting tools are rarely perfectly sharp, this edge radius effect can be an important parameter in inducing residual stresses into the machined subsurface.

There are various quantitative and qualitative techniques to measure residual stresses. They are mainly classified into destructive and nondestructive methods. The various residual stress-measuring methods are:

<i>X-ray</i>	<i>Hole drilling</i>
<i>Neutron diffraction</i>	<i>Deflection</i>
<i>Ultrasonic</i>	<i>Sectioning</i>
<i>Magnetic</i>	

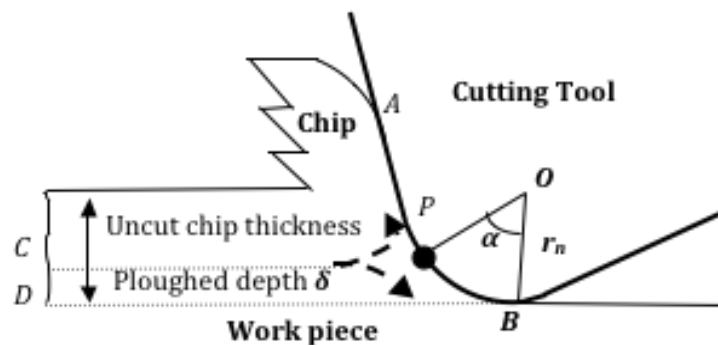


Fig 1.1 Ploughing phenomenon [4]



### 1.3 Thesis Overview

The role of cutting fluid's usage in machining has been reevaluated over the years. Considerable research work attempted to address issues related to environment, health, cost, and part performance. However, the influence of targeted application of minimal quantities of coolant and/or lubricant with compressed air jet is limited. An experimental study involving facing of medium carbon steel (AISI 1045) was conducted to address the tribological effects (forces, chip flow, chip morphology, tool chip contact area, and surface roughness) and surface integrity (residual stresses) in machined surfaces. Tests of flat-faced, uncoated cutting tools under different cutting fluid application conditions along with dry machining were conducted. The procedures used to test the above-mentioned parameters are explained in detail in Chapter 3.

Targeted application of cutting fluid produced interesting near surface residual stresses, especially when a certain amount of coolant only (60 ml/hr) (under compressed air jet 0.6 MPa) was directed onto the tool flank face. Coolant on the flank face induced compressive residual stresses while all other tests induced tensile residual stresses. This study discusses the results associated with different cutting fluid combinations application. It further emphasizes the importance of the location on the tool surface at which the minimal quantity cutting fluid is disposed and its effects on the surface integrity.

This work emphasizes the detrimental influence of flood machining on the environment and the significant advantages of minimum quantity cutting fluid application in Chapter 1. Residual stress introduction is also briefly given in the same chapter. A detailed technical review of previous research is provided in Chapter 2. Available

literature review disclosed the need for conducting this study. Chapter 3 focuses on the experimental plan and set up, explaining the design of a Minimum Quantity Cutting Fluid (MQCF) dispensing system and steps involved in residual stress measurement. It also contains the procedures employed to test the triobological effects (forces, chip flow prediction, surface roughness). Chapter 4 presents the results of a series of machining experiments that explains the targeted cutting fluid application effects on triobological and residual stress effects. The importance of the positive effects of directing the coolant onto the tool flank face is discussed here. Chapter 5 sums up the work accomplished and present the recommendations for future research.

#### 1.4 References

1. ASM Specialty Handbook - Carbon and Alloy Steels, edited by J.R. Davis, Davis & Associates, ASM International, Metals Park, OH, (1996).
2. Field, M., Kahles, J.F. (1971) 'Review of surface integrity of machined components', *Annals of the CIRP*, Vol. 20(2), pp.153-162.
3. Ghatikar, V. (2010) 'Design of Minimal Quantity Cutting Fluid dispensing system for sustainable machining'. *MS Thesis, University of Utah*.
4. Guo, Y.B., Anurag, S. and Jawahir, I.S. (2009) 'A novel hybrid predictive model and validation of unique hook-shaped residual stress profiles in hard turning', *Annals of CIRP – Manufacturing Technology*, Vol. 58, pp.81-84.
5. Jayal, A. D. (2006) 'An experimental investigation of the effects of cutting fluid application on machining performance', *Phd dissertation, University of Utah*.
6. Klocke, F. and Eisenblatter, G. 1997, 'Dry Cutting', *Annals of CIRP*, Vol. 46(20), pp. 519-526.
7. Metals Handbook, Vol.1 - Properties and Selection: Irons, Steels, and High-Performance Alloys, ASM International 10th Ed. 1990.
8. Okushima, K. and Kakino, Y. (1971) 'The residual stress produced by metal cutting', *Annals of CIRP*, Vol. 20(1), pp. 13-14.
9. Shaw, M. C. (1984) *Metal Cutting Principles*, Oxford University Press.
10. Trent, E. M. (1991) *Metal Cutting*, 3<sup>rd</sup> Edition, Butterworth-Heinemann Ltd.

## **CHAPTER 2**

### **BACKGROUND**

In recent years, there has been a need for renewed research and analysis on the effects of new tool materials and coatings on machining performance, tool life, and workpiece surface quality in terms of geometrical accuracy and residual stresses.

Machining performance in metal cutting operations can be gauged with the amount of heat generated and the friction between tool and work material (chip). Cutting fluids, including coolants and/or lubricants delivered with compressed air jet, help in minimizing the temperature and friction in the cutting zone and help in enhancing tool life. However, the indiscriminate and uncontrolled use of cutting fluids causes severe environmental problems and increased costs associated with fluid filtration and associated health concerns for workers exposed to cutting fluid particulates. This fact leads to an attempt which consists of directing the flow to particular contact regions and enhancing the performance of the machining operation. The following technical review of previous research on the effects of cutting fluid application on surface integrity and tribological aspects establishes the need for pursuing the research presented in this thesis.

#### **2.1 Minimum Quantity Cooling and Lubrication**

The Occupational Safety and Health Administration (OSHA) has regulated the usage of cutting fluids in the last 20 years, which has resulted in lowering of the

permissible exposure limit from  $5 \text{ mg/m}^3$  to  $0.5 \text{ mg/m}^3$ . Industries heavily associated with machining have also been working towards reducing costs and improving productivity [2], which has led to a heightened interest towards dry or minimum quantity cooling and/or lubrication. Controlling the amount of cutting fluid delivered can enhance specific machining performance with decreasing costs and environmental impacts.

In some cutting processes, dry cutting has been implemented as a possible alternative to the use of flood cutting fluid, by using developed tool materials that are resistant to high temperatures and wear. This option turns out to be very expensive due to the application of specially designed, high wear resistant cutting tools (grooves, chip breakers, heat resistant material). Also, since the tool life is very short, dry cutting cannot be used with high depth of cut [11].

In minimum quantity cooling and/or lubrication, coolant and/or oil are applied, respectively, with a compressed air stream as a mist to the cutting tool and/or the workpiece, which is being machined at small fluid volumes of 5-100mL/h. The straight oils are usually chosen as lubricants for their higher lubricity compared to mineral oils. It has been hypothesized that the mechanism involved for the cutting fluid to reach the tool-chip interface is molecular diffusion [7] and hence, cutting fluids of small molecular size at high pressures have been recommended for application in machining.

Thepsonthi (2009) stated that application of pulsed-jet produces beneficial effects in terms of cutting forces, surface roughness, tool wear, and cutting temperature [38].

There are some explanations in the literature on the mechanism of cutting fluid penetration and action. The cutting fluid jet lubricates the tool-chip and tool-work-piece interfaces. During the process, the freshly generated metal surfaces of the chip produce a

metallic sulfide film, due to the chemical reaction caused by sulfur content in the cutting fluid, which is an extreme-pressure additive [12]. The sulfide film has lower shear strength than the chip material that helps in reducing friction and cutting forces. This chemical reaction thwarts welding action between the surfaces in contact, and hence avoids the mechanical peel-off of the tool material [9].

Wakabayashi et al. (1998) showed that ester dispensed onto the cutting tool decomposes to carboxylic acid and alcohol and the carboxylic acid forms a chemisorbed film with lubricity [40]. Itoigawa et al. (2006) worked on Minimum Quantity Lubrication (MQL) and MQL with water droplets (OoW - oil film on water droplets) and found that cooling ability is important for dimensional accuracy of machined workpieces and tribological phenomena between the tool-work-piece interface, such as adhesion [19]. They also concluded that the water droplets ensure that the lubricant coating deposits and spreads over the work zone due to the droplets' inertia.

However, it was reported [27, 35] that lubricant reaches the tool face in end milling easier than in turning, which implies that MQL is more effective in end milling. The interrupted nature of the milling processes possibly enhances lubricant access and action. This calls for additional research on finding a method to have the cutting fluid reach the tool rake face in a continuous operation such as turning. The potential benefits are improvements in tribological and machining performance. This thesis attempts to address some of these questions by evaluating lubricant and coolant access when dispersed in minimal amounts.

Pigott and Colwell (1952) first discussed the use of high-pressure cutting fluid with high-speed steel tools in steel turning, since the penetration capacity of lubricant at

low velocity does not allow it to reach the cutting edge, which favors the formation of a built up edge [33]. Also, the amount of cutting fluid dispensed/sprayed could be reduced with high-pressure jet application [22].

In an interesting contrast, while machining titanium alloy tool life increased with the use of a high-pressure cooling system, when machining nickel alloy, the same system reduced the tool life due to notch wear [28]. Ezugwu (2004) pointed that materials like Inconel 718, which have low machinability due to low thermal conductivity and high temperature, compressive stress on the cutting edge leads to tool wear [13]. Cutting fluid at high pressure increases lubrication capacity and reduces the temperature in all the interfaces. When a range of high jets of cutting fluid of up to 15 MPa were applied while cutting with an uncoated carbide tool, there was a considerable increase in tool life. On the other hand, when the pressure was increased to 20.3 MPa, the tool life decreased. This decrease in tool life was attributed to the critical boiling action of the coolant at the tool edge. It was possible that the tool surface was washed away faster with such high jet speed by amplifying the rate of boiling and cutting down the heat transfer [14].

There are three possible directions of cutting fluid application in a cutting operation, which have their own advantages and disadvantages based on the cutting conditions:

- Chip-tool interface (tool rake face)
- Workpiece-tool interface (tool flank face)
- Onto the top surface of the chip

During cutting, a seizure (or sticking) zone occurs in the chip-tool interface, due to the high stress on the tool rake face [4]. Here, the chip velocity approaches zero and

the actual contact area is equal to the apparent area. High heat is generated in this area because of the large amount of shearing inside the chip and above the interface. Due to complete contact between the tool and the chip, it is almost not possible for the fluid to penetrate between the tool and the chip [39]. Machado et al. (1994), on the other hand, suggested that the seizure zone could be marginally decreased if fluid is directed at high pressure [28]. The sliding zone surrounding the sticking zone can also be reduced with high-pressure fluid.

The airflow due to the workpiece rotation hinders the proper penetration of the fluid towards the workpiece-tool interface. At higher cutting speeds, it becomes more difficult for the fluid to reach the cutting zone [3,11]. Consequently, lower cutting speeds may increase tool life.

Applying the fluid on top of the chip does not perform any lubrication action; instead, it cools down the chip to a larger extent than the workpiece and the tool, resulting in harder chips, lower tool life, and increased tool wear [3,11].

## 2.2 Chip Morphology

Tool-chip contact governs the movement of the chip from the tool rake face along with the chip curl or the deformation imparted to the chip [4]. Initially, chip flow over the tool rake face was assumed to be perpendicular to the major axis of the projected area of cut [8]. Later, a relation was introduced stating that the chip-flow angle will equal the inclination angle (Stabler's flow rule). This further led to modeling the mechanics involved in the prediction of cutting forces and chip flow angle [1,37]. Other models have been consistently updated with new geometric features, validated by experimental work



by various researchers through the years [1,37]. Balaji and Jawahir (1999) illustrated how the nose radius (0.8 mm) dominates the straight portion of the small depth of cut (1.2 mm) and leads to the formation of side curled chips [4].

The application of cutting fluid has a limited ability to significantly influence the seized region of interfacial tool-chip contact length [21]. Ezugwu et al. (2005) confirmed that by using the high-pressure cutting fluid, contact length between chip and tool decreased, eventually decreasing temperature [14].

### 2.3 Surface Roughness

Qualitative excellence of the finished part is a desired property in a manufacturing process. The finishing process (turning) has a very large effect on the final surface texture. Surface roughness is the geometric deviation of the final surface from the desired surface texture. This deviation of the final surface is mainly due to workpiece-tool interface and partly due to factors like tool wear, machine tool vibration, etc.

The selection of the cutting fluid is usually based on reduced thermal deformation, heat transfer performance, lubrication performance, and chip flushing. Liu et al. (2009) reported that spraying oil/water emulsion onto the flank face produced significantly lower surface roughness. The biodegradable vegetable oil molecules, sprayed between tool and chip, are absorbed into the area between the tool and workpiece, forming a lubricating film. The cutting fluid also cools the workpiece and tool region, and hence leads to the reduction in friction of chip-tool and tool-workpiece. The deformation of the material in the cutting zone is reduced, and the bonding degrees between chip and tool rake is reduced, thus lowering the value of surface roughness. This cutting fluid deposition also improves the chip-breaking ability, preventing the chips

from winding around the workpiece and hence effectively improving the workpiece surface roughness [26].

#### 2.4 Residual Stresses

The mechanisms behind machining-induced residual stresses were reviewed and presented by various research studies since the 1950s [6,15,17,23,24]. In a machining process, mechanical loading, thermal gradient, and phase transformation cause residual stresses due to inhomogeneous material deformation [16].

Surface residual stresses affect the functional aspects of the final part such as fatigue life, corrosion resistance, and wear resistance. The tensile or compressive stresses developed during the machining process are influenced by the cutting parameters, tool geometry, and nature of the worked material [3]. The residual stress profile into the material can be defined as a function of the process parameters such as the cutting speed, feed rate, and depth of cut [9,10,18,20,29,30]. Prediction of residual stresses is difficult as the residual stresses vary non-uniformly over the machined surface [34]. Hence, this remains an area of critical importance since considering the residual stresses induced in the machining process is essential in the performance of the final product.

Henriksen et al. (1951) conducted lengthwise machining by planning and shaping various carbon steels at different cutting conditions in a dry environment and concluded that stress concentration lowers resistance to wear and corrosion, which further leads to fatigue or hairline cracks [16,17]. Bailey et al. (1976) determined the subsurface plastic strain in machining copper and 18% nickel maraging steel orthogonally by using a microtome (diamond indenter) to emboss a grid and then studying the distortion of the array [5]. It was suggested that subsurface plastic strains are produced due to the mode of

deformation of material during chip formation and adhesion between the tool clearance face and freshly machined workpiece surface. These plastic strains can influence the residual stress distribution within the surface [5].

Okushima et al. (1971) conducted a theoretical analysis on the causes of residual stresses by comparing the results of residual stresses using finite element methods. These were measured by X-ray diffraction method, by turning 0.45% carbon plain steel at 2 mm depth of cut, 0.125 mm/rev feed, and 0.5 mm nose radius carbide tool at various cutting speeds [31]. It was found that the magnitudes of residual stresses in oblique cutting are smaller by 10 to 20 kg/mm<sup>2</sup> than those in orthogonal cutting. The machined surface is produced by the major cutting edge in orthogonal cutting, while in conventional cutting, it is produced by the minor cutting edge where it involves smaller localized depth of cut at the last portion of the rounded tool corner. At this tool-work contact surface, the tool largely performs a burnishing action, which can compress the machined surface sublayer. It was also investigated that mild cutting conditions like low cutting speed, large vertical ploughing force, small frictional force on the tool relief angle, and low temperature rise tends to decrease tensile residual stress in the subsurface layer of the work piece [31].

Outeiro and Dias (2006) worked on 316L and 1045 steel and evaluated the variation of residual stresses and work hardening between coated and uncoated cutting tools. They determined that uncoated tools produce lower superficial residual stresses, lower tensile layer thickness, lower subsurface tensile stresses, and lesser work hardening than coated tools as the coated tools conduct less heat (coated tools have lower thermal conductivity than uncoated carbide tools) [32]. Attanasio et al. (2009) observed that the

use of low tool edge radius (sharp tool) and Minimum Quantity Lubrication (MQL) on AISI 1045 steel reduced the value of minimum principal residual stresses [3].

It was demonstrated that a worn tool could generate tensile residual stresses, which is influenced by the flank tool wear [24,25].

All this background literature is a motivating factor in this thesis to test the hypothesis of directed cutting fluid effects on surface integrity by directing cutting fluid to different cutting zones: tool rake face and tool flank face.

## 2.5 References

1. Armarego, E. J. A. and Samaranayake, P. (1999) 'Performance prediction models for turning with rounded corner plane faced lathe tools. I. Theoretical development', *Machining Science and Technology*, Vol. 3(2), pp. 143-172.
2. Astakhov, V.P. (2010) 'Metal cutting theory foundations of near-dry (MQL) machining', *Int. J. Machining and Machinability of Materials*, Vol. 7, Nos. 1/2, pp.1-16.
3. Attanasio, A., Ceretti, E., Gelfi, M. and Giardini, C. (2009) 'Experimental evaluation of lubricant influence on residual stress in turning operations', *Int. J. Machining and Machinability of Materials*, Vol. 6 (1/2), pp. 106-119.
4. Balaji, A.K., G. Sreeram, I.S. Jawahir and E. Lenz, (1999) 'The effects of cutting tool thermal conductivity on tool-chip contact length and cyclic chip formation in machining with grooved tools', *Annals of the CIRP*, Vol. 48(1), pp. 33-38.
5. Bailey, J. A. and Jeelani, S. (1976) "Determination of Subsurface Plastic Strain in Machining Using an Embossed Grid", *Wear*, 36, pp. 199-206.
6. Brinksmeier, E., Cammett, J.T, Konig, W., Leskovar, P., Peters, J. and Tonshoff, H.K. (1982) 'Residual stresses-measurement and causes in machining processes', *Annals of CIRP*, Vol. 31(2), pp.491-510.
7. Cassin, C. and Boothroyd, G. 1965, 'The Lubrication Action of Cutting Fluids', *Journal of Mechanical Engineering Science*, Vol. 7(1), pp. 67-81.
8. Colwell, L. V. (1954) 'Predicting the angle of chip flow for single point cutting tools', *Trans. ASME*, Vol. 75(B2), pp. 199-204.
9. Dahlman, P. and Escursell, M. 2004, 'High-Pressure Jet-Assisted Cooling: A New Possibility of Near Net Shape Turning of Decarburized Steel', *International Journal of Machine Tools and Manufacture*, Vol. 44(1), pp. 109-115.
10. Dahlman, P., Gunnberg, F. and Jacobsen, M. (2004) 'The influence of rake angle, cutting feed and cutting depth on residual stresses', *Journal of Materials Processing Technology*, Vol. 147, pp.181-184.
11. Diniz, A. E. and Micaroni, R. (2007) 'Influence of the Direction and Flow Rate of the Cutting Fluid on Tool Life in Turning Process of AISI 1045 Steel', *Int. J of Machine Tools AAND MAnufacture*, Vol. 47, pp.247-254.
12. Drazda, T. J. and Wick, C. 1983, 'Machining: Tool and Manufacturing Engineering Handbook', *Society of Manufacturing Engineering (SME)*, Vol. 1.

13. Ezugwu, E. O. and Bonney, J. (2004) 'Effect of High-Pressure Coolant Supply when Machining Nickel-base, Inconel 718, Alloy with Coated Carbide Tools', *J of Materials Processing Technology*, Vol. 153-154, pp. 1045-1050.
14. Ezugwu, E. O., Da Silva, R. B., Bonney, j. and Machado, A. R. (2005) 'Evaluation of the performance of CBN tools when turning Ti-6Al-4V alloy with high pressure coolant supplies', *Int. J of Machine Tools and Manufacture*, Vol. 45, pp. 1009-1014.
15. Field, M., Kahles, J.F. (1971) 'Review of surface integrity of machined componenets', *Annals of the CIRP*, Vol. 20(2), pp.153-162.
16. Guo, Y.B., Li, W. and Jawahir, I.S. (2009) 'Surface integrity characterization and prediction in machining of hardened and difficult-to-machine alloys: A state-of-art research review and analysis', *Machining Science and Technology*, Vol. 13, pp.437-470.
17. Henriksen, E.K. (1951) 'Residual stresses in machined surfaces', *Transactions of ASME*, Vol. 73, pp. 69-76.
18. Hua, J., Shivpuri, r., Cheng, X., Bedekar, V., Matsumoto, Y., Hashimoto, F. and Watkins, T. R. (2005) 'Effect of feed rate, workpiece hardness and cutting edge on subsurface residual stress in the hard turning of bearing steel using chamfer + hone cutting edge geometry', *Material Science and Engineering A*, Vol. 394, pp.238-248.
19. Itoigawa, F., Childs, T. H. C., Nakamura, T. and Belluco, W. (2006) 'Effects and Mechanisms in Minimal Quantity Lubrication Machining of Aluminium Alloy', *WEAR*, Vol. 260, pp. 339-344.
20. Jacobson, M., Dahlman, P. and Gunnberg, F. (2002) 'Cutting speed influence on surface integrity of hard turned bainite steel', *Journal of Materials Processing Technology*, Vol. 128, pp.318-323.
21. Jayal, A. D. (2006) 'An experimental investigation of the effects of cutting fluid application on machining performance', *Phd dissertation, University of Utah*.
22. Kaminski, J. and Alvelid, B. (2000) 'Temperature Reduction in the Cutting Zone in Water-jet assisted Turning', *J of Materials Processing Technology*, Vol. 106, pp. 68-73.
23. Koster, W.P., Field, M., Fritz, L.J., Gatto, L.R. and Kahles, J.F. (1970) 'Surface integrity of machined structural components', *Technical Report AFML-TR-70-11*, Metcut Research Associates, Inc.

24. Liu, C.R. and Barash, M.M. (1982) 'Variables governing patterns of mechanical residual stress in a machined surface', *Transactions of ASME*, Vol. 104(3), pp.257-264.
25. Liu, M., Takagi, J. I. and Tsukuda, A. (2004) 'Effect of tool nose radius and tool wear in residual stress distribution in hard turning of bearing steel', *Journal of Materials Processing Technology*, Vol. 150, pp. 234-241.
26. Liu, Y., Wang, A., Wang, B. and Liu, Z. (2009) 'Experimental study on the effects of oil/water emulsion on machining stainless steel', *International Technology and Innovation Conference 2009 (ITIC 2009)*, pp. 1-4.
27. Lopez de Lacalle, L. N., Lamikiz, A., Sanchez, J. A. and Cabanes, I. (2001) 'Cutting Conditions and Tool Optimization in the High-Speed Milling of Aluminium Alloys', *Proc. IMechE, Part B*, Vol. 215, pp. 1257-1269.
28. Machado, A. R. and Walbank, J. (1994) 'The Effects of a High Pressure Coolant Jet on Machining', *Proceedings of the Institution of Mechanical Engineers, Part B: J of Engineering Manufacture*, Vol. 208, pp.
29. Matsumoto, Y., Hashimoto, F. and Lahoti, G. (1999) 'Surface integrity generated by precision hard turning', *Annals of CIRP*, Vol. 48, No. 1, pp.59-62.
30. Mittal, S. and Liu, C. R. (1998) 'A method of modeling residual stresses in superfinishing hard turning', *Wear*, Vol. 218, pp. 21-33.
31. Okushima, K. and Kakino, Y. (1971) "The Residual Stress Produced by Metal Cutting", *Annals of CIRP*, Vol. 20 (1), pp.13-14.
32. Outeiro, J. C. and Dias, A. M. (2006) 'Influence of Work Material Properties on Residual Stresses and Work Hardening Induced by Machining', *Materials Science Forum*, Vol. 524-525, pp. 575-580.
33. Pigott, R. J. S. and Colwell, A. T. (1952) 'Hi-jet System for Increasing Tool Life', *SAE Quarterly Transactions*, Vol. 6(2), pp. 547-558.
34. Prevey, P.S. and Field, M. (1975) 'Variation in surface stress due to metal removal', *Annals of the CIRP*, Vol. 24(1), pp.497-501.
35. Rahman, M., Senthil Kumar, A. and Manzoor-Ul-Salam, (2001) 'Evaluation of Minimal Quantities of Lubricant in End Milling', *Adv. Manuf. Technol.*, Vol. 18, pp. 235-241.
36. Ramesh, A., Melkote, S. N., Allard, S. N., Riester, L. and Watkins, T. R. (2005) 'Analysis of White Layers Formed in Hard Turning of AISI 52100 Steel', *Materials Science Engineering A*, Vol. 390, pp. 88-97.

37. Redetzky, M., Balaji, A.K., Jawahir, I.S. (1999) 'Predictive modeling of cutting forces and chip flow in machining with nose radius tools', *Proc. 2nd CIRP Int. Workshop on Modeling of Machining Operations*, Nantes, France, pp.160-180.
38. Thepsonthi, T., Hamdi, M. and Mitsui, K. (2009) 'Investigation into Minimal-Cutting-Fluid Application in High-Speed Milling of Hardened Steel Using Carbide Mills', *International Journal of Machine Tools and Manufacture*, Vol. 49(2), pp. 156-162.
39. Trent, E. M. (1991) 'Metal Cutting', *Butterworths-Heinemann, Oxford*.
40. Wakabayashi, T., Sato, H. and Inasaki, I. (1998) 'Turning using Extremely Small Amount of Cutting Fluid', *JSME Int. J. Ser. C*, Vol. 41(1), pp. 143-148.



## **CHAPTER 3**

### **EXPERIMENTAL PLAN AND SETUP**

This chapter presents the methodology used for conducting the experiments, including the design and fabrication of the minimum quantity cutting fluid dispensing system. The incremental hole-drilling strain-gage method used to measure residual stresses on the machined surfaces is also demonstrated in this chapter.

#### 3.1 Experimental Plan

The experiments were planned in view of studying the triobological and surface integrity effects while facing medium-carbon steel with flat-faced uncoated tools. The variables employed in this work are different cutting fluid combinations and proportions dispensed onto the tool rake/flank face. The triobological parameters that were studied in this thesis are forces, predicted chip flow angle, chip morphology, tool-chip contact area, and surface roughness. Residual stresses were measured and analyzed as part of surface integrity study.

The experiment was setup to machine (face) cold drawn, medium-carbon AISI 1045 steel. The composition of AISI 1045 steel is provided in Table 3.1. Steel cylindrical bars of 4" (101.6 mm) diameter and 2" (50.8 mm) width were machined by means of the facing operation using straight edge, single point cutting tools.

Table 3.1 Chemical Composition of AISI 1045 steel [5].

Element	Carbon, C	Manganese, Mn	Phosphorous, P	Sulphur, S
Weight %	0.43 – 0.50	0.60 – 0.90	0.04 (max)	0.05 (max)

Tests were conducted on a HAAS SL-20 CNC turning center under fixed cutting conditions and varying cutting fluid combinations.

Flat-faced, uncoated cemented tungsten carbide tools were selected to study the cutting fluid combination effects on basic tool surface topography and surface integrity. The selected tools were triangular shaped (TNMA) with an included angle of  $60^\circ$ , inscribed circle diameter of 0.5" (12.7 mm) with a thickness of 0.1875" (4.7625 mm) and a nose radius of 0.03125" (0.79375 mm). The selected carbide tool, TNMA grade K68 (Manufacturer: Kennametal) has a composition of hard, low binder content, unalloyed, WC/Co fine-grained grade with a well-controlled grain structure for minimal pits and flaws that contributes to long and reliable service. Tests were conducted at a cutting speed of  $v = 225$  m/min, feed rate of  $f = 0.1$  mm/rev, and a depth of cut of  $a_p = 1.2$  mm. The cutting conditions were selected based on previous work done on AISI 1045 steel machining [9].

The tool holding fixture was instrumented with a triaxial measurement Piezoelectric sensor/transducer - a Kistler® 9121 three-component dynamometer interfaced with Kistler® charge amplifiers (5010) connected to a National Instruments Labview™-based data acquisition system PCI 6703 to measure the feed ( $F_f$ ), radial ( $F_r$ ), and main cutting ( $F_c$ ) components of force.

The cutting fluid was applied in the form of an approximately overhead jet directed towards the tool rake/flank face, at about 2 mm from the cutting edge. A conical spray angle of 15 – 20° ensured CF delivery to all the zones of the tool rake face and the flank face.

The experimental plan is schematically shown in Figure 3.1 with the direction of cutting fluid dispensed onto different cutting tool surfaces (tool rake face and tool flank face). The front, side and isometric views of the experimental setup show how the cutting fluid dispensing nozzles are placed close to the tool.

The lubricant used for the experiments was soluble oil concentrate (Coolube 2210) in 0.6 MPa (87 psi) air supply routed from UNIST's uni-MAX coolubricator. When the lubricant is sent out of its source tube, air and lubricant mixture is formed at the tip of the nozzle, which is then dispensed in the form of an aerosol mist.

The coolant (water, in this thesis) was supplied using a formerly designed and fabricated minimum quantity cutting fluid dispensing system [7] that allows simultaneous application of multiple fluids. In this case air and coolant (water) were used as a medium, where the water droplets are integrated with air at the tip of the nozzle directly before dispensing. The coolant amounts were calibrated via programming instructions using LabView, while the air supply was 0.6343 MPa (92 psi) throughout all the tests. Depending on the amount of voltage input, the water (coolant) amount was regulated.

Figure 3.2 gives a schematic view of the Minimum Quantity Cutting Fluid dispensing system and the cutting fluid combinations are listed in the Table 3.2.

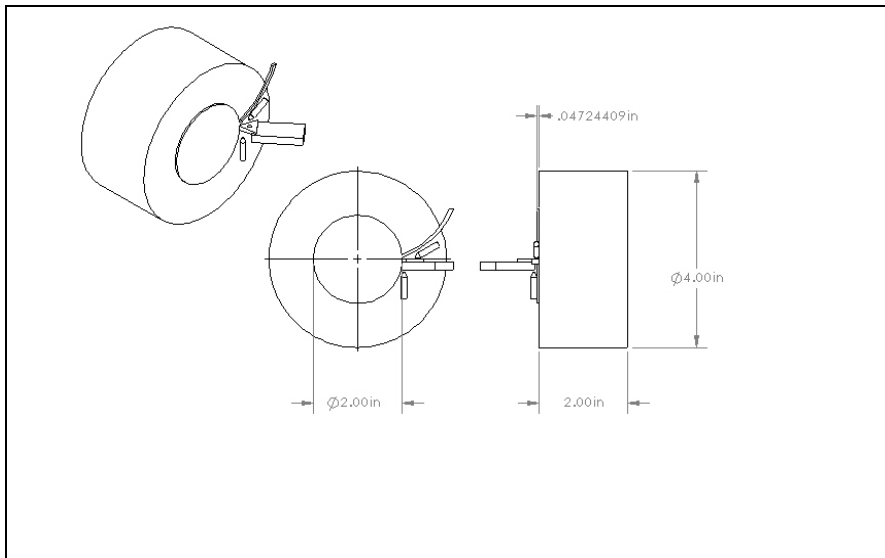


Figure 3.1 Experimental setup

Table 3.2 Cutting fluid combinations

100% = 60 ml/hr, 75% = 45 ml/hr, 50% = 30 ml/hr, 25% = 15 ml/hr  
 Coolant: water, Lubricant: soluble oil concentrate (Coolube 2210)

Experiment	% of Coolant	% of Lubricant
1 (Dry)	0	0
2 (rake face)	100	0
3 (rake face)	75	25
4 (rake face)	50	50
5 (rake face)	25	75
6 (rake face)	0	100
7 (flank face)	100	0

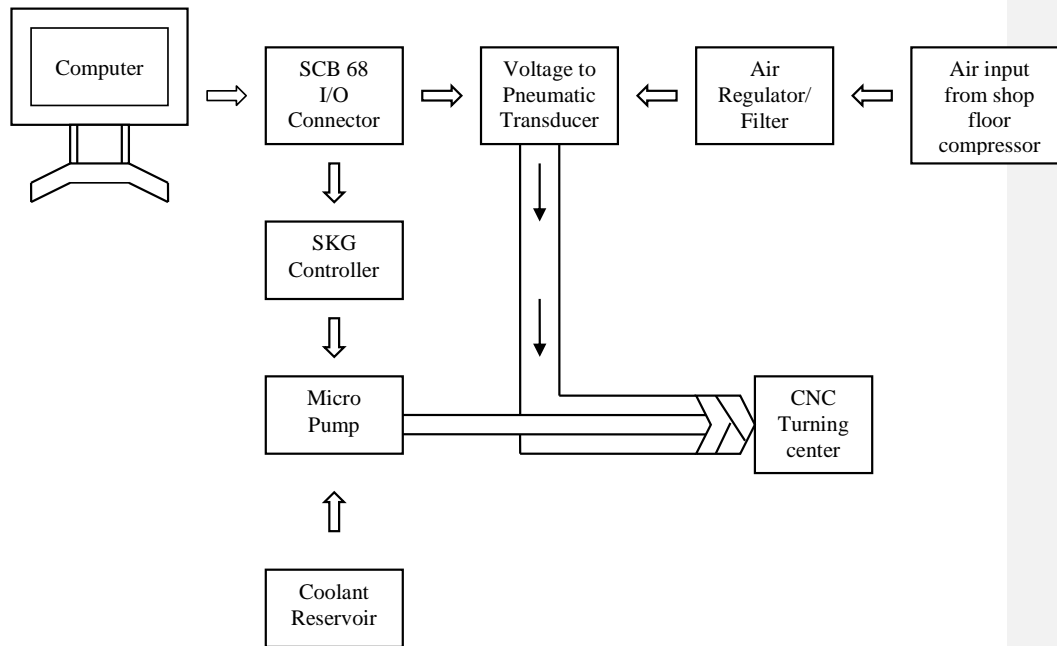


Figure 3.2 Flowchart of the Minimum Quantity Cutting Fluid (MQCF) dispensing system

### 3.2 Minimum Quantity Cutting Fluid Dispensing System

The components involved in the minimum quantity cutting fluid dispensing system are as follows:

1. This component utilizes closed-loop pressure feedback circuitry, and it provides precise, stable pressure outputs to final control devices. It has 0-10 V DC signal input range. The input range for this transducer was 0~130 psi while the output range was 0~100 psi. The transducer complies with the limitations of the compressor on the shop floor, which delivered an input pressure of air limited to a maximum of 130 psi. The transducer weighs 13.0 oz (0.4 Kg), is 3.69" x 2.94" x 1.5" in size and has ¼" NPT port size for air and ½" for the electrical port.

2. An external AC to DC power supply was used, since the transducer required a power supply of at least 7 V DC.
3. The transducer requires an air supply filtered under 40 microns; for this, [a SMC – Integrated AW 30 series air filter](#) with a regulator was used to connect the shop floor compressor line and the transducer. In addition, the air regulator also protected the transducer against any sudden surge in pressure from the direct source, i.e., the compressor line.
4. Micro-Annular Gear Pump: The HNP Mikrosysteme GmbH micropump, m2r - 2521 was used to control the fluid flow rate, thereby enabling a wide range of flow types ranging from droplets to the aerosol flow. This positive displacement pump satisfied the design constraints and interfaced well with the software. The low-pressure series pump weighed 56 grams with 13 mm (diameter) 5 mm (length) in size. The maximum flow rate of the pump was 9 ml/min, while the minimum flow rate could go down to 0.1 ml/min with the smallest dosage volume of 0.25  $\mu$ l. The pump's maximum speed was 6000 rpm and the allowed viscosity range was 0.3 to 100 mPa.
5. A SK-G controller that converts an electronic signal to a mechanical loading input compatible with the pump functioning was used to let the pump interface with the CPU. This controller required a 24 DC power supply with an analog input signal of 0 to 10 V DC and it could work under various rpm ranges as low as 10 for droplets or aerosol flow dispensing. The controller weighed approximately 35 grams and was 68 mm x 57 mm x 24 mm in size.

6. A National Instruments Peripheral Component Interconnect (PCI)-6703, 16 channel analog output card was used to convert the digital current or voltage value to an analog signal in order to integrate the hardware components with the CPU and hence the LabView program. 16 channels in the PCI card resemble 16 voltage output ports through which 16 different hardware components can be accessed.
7. A SCB-68 connector block was used to wire the mechanical components with the PCI – 6703. This connector block has a 68-pin connection, noise reduction, and shielded I/O block.
8. SMC one-touch push type connectors and pipes were used to install, connect, and remove the pipes as required. These connectors operate up to a maximum pressure of 150 psi.

This system was built as part of a different MS thesis [7] but the first implementation of such a system to evaluate the effects of differing fluid dispensing rates and target directions has been implemented in this thesis work.

Working principle: The devices described above are connected as shown in Figure 3.2., based on the LabView simulator instructions. The National Instruments PCI 6703 DAQ card sends analog signals (0-10 V DC) to the SCB-68 connector to regulate the flow rate of both air and cutting fluid. The code is developed such that the magnitude of the voltage input varies the fluid pressure.

The micropump is connected to the coolant reservoir at the source pin and the delivery pin is connected to the SKG controller, which obtains its regulating signal from the SCB-68 connector. Air from the shop floor compressor is cleaned and filtered in the

air regulator and then sent into the voltage-to-pneumatic transducer. Air pressure is calibrated in the transducer, passed into the pressure gage, and directed into the outer part (8 mm in diameter) of a concentric tube while the inner tube (3 mm in diameter) carries the cutting fluid.

Air mixes with the cutting fluid at the tip of the concentric tube in the nozzle and the mixture is directed onto the cutting tool in the form of aerosols. If required, droplets of cutting fluid can be directed if the pressurized air is shut off.

### 3.3 Measurement of Tribological Parameters

#### 3.3.1 Prediction of Chip Flow Angle

The chip flow angles for the cutting conditions tested in this thesis were predicted using an algorithm from a comprehensive predictive model for cutting forces and chip flow in machining with nose radius tools [2,12]. The inputs for the model were cutting conditions (feed, depth of cut) and the three force values (feed force, radial force, and main cutting force), which are retained while machining.

#### 3.3.2 Tool-Chip Contact Area

Scanning Electron Microscope (SEM) – 100x imaging analysis was undertaken on the flat-faced uncoated carbide tool after facing 1045 carbon steel cylindrical bars. This microscope uses electrons to form an image. The SEM has a large depth of field, which allows a large amount of the sample to be in focus at once. The SEM also produces images of high resolution, which means that closely spaced features can be examined at a high magnification. The analysis was conducted to determine the extent of tool-chip contact area for each case of cutting fluid application at the targeted cutting tool face.



### 3.3.3 Chip Morphology

The basic chip morphology was studied via a visual examination of the chips obtained while machining. The chip flow and chip curl mechanisms were observed in each case of cutting fluid application. Chip flow usually constitutes chip side-flow and chip back-flow, while chip curl consists of chip up-curl and chip side-curl [3].

### 3.3.4 Surface Roughness

The average surface roughness values ( $R_a$ ) of the machined work pieces were measured using a Zygo® NewView 5000 series optical interferometry-based surface profilometer. A profilometer uses a diamond stylus (which works like a phonograph) to measure a subject's length or depth (profile), usually at the micron and nanometer levels. This optical surface profilometer, with the help of comprehensive MetroPro™ metrology software, characterizes and quantifies surface roughness, step height, and critical dimensions with precision and accuracy. Image zoom of 2x and 20x objective were used. Surface roughness values ( $R_a$ ) were obtained at three different locations on the machined work pieces and an average of these three values was considered for the analysis. Theoretical machining surface roughness ( $R_a$ ) is  $f^2/32NR$ , where  $f$  is feed and  $NR$  is nose radius [8].

### 3.4 Residual Stress Measurement

The hole-drilling strain-gage method was used to measure the residual stresses induced in the machined work pieces. The basic principle to measure the residual stress and implement the calculation method was first proposed by Mathar 1934 [10]. The procedure briefly included the following steps:

Strain-gage installation: The strain-gage rosettes CEA-06-062UL-120, which are manufactured by Vishay Micro-Measurements [14,15], were used for the residual strain measurement. Figure 3.4 shows an example strain-gage rosette. This strain-gage was chosen for the experiments based on industrial recommendations in relation with the work material and cutting conditions. The thin, flexible gages with cast polyimide backing and large rigged copper coated solder tabs allow optimum capability for direct attachment of the lead wire. The foil is made of Constantan alloy in self-temperature-compensated form (CEA).

The self-temperature-compensation number (06) is the approximate thermal expansion coefficient ( $6.7\text{ppm}/^{\circ}\text{F}$ ) of the structural material (steel 10XX) on which the gage is used. The gage length used for the experiments is 0.062 inches (062).

The letters 'UL' of the type of strain-gage rosette used in this work designate the grid and tab geometry. The resistance of the strain-gage used is  $120\pm 0.4\%$  ohms [15].

#### 3.4.1 Hole Drilling and Strains Acquisition

The hole-drilling strain-gage method described in ASTM Standard E837 is one of the most widely used practical techniques to determine residual stresses [6]. In this method, a specially configured strain-gage rosette is bonded to the surface of interest. A shallow hole with incremental depth is drilled into the structure through the center of the gage with the help of a precision drilling apparatus. Residual stresses are determined from the measured strains from the immediate vicinity of the hole. The hole-drilling experiments were conducted on a three-axis CNC-VFE Vertical Machining Center with 765mm x 408mm x 508mm travel and 20 HP spindle motor.

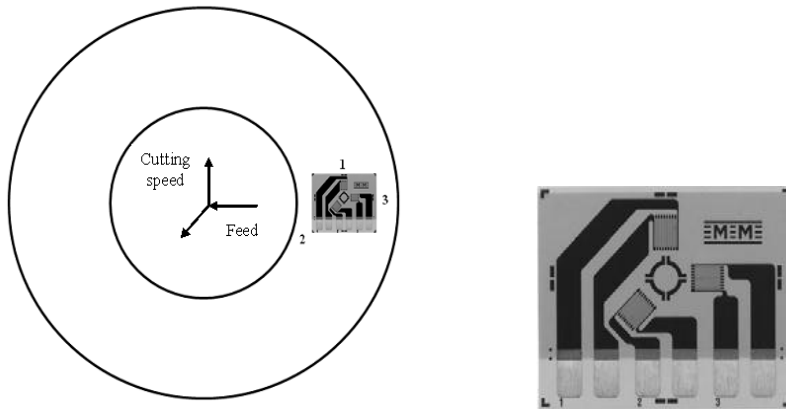


Figure 3.4: Strain-gage rosette, directions [4].

Experiments were conducted at a spindle speed of 2000 rpm and a feed rate of 1 inch/min. High Speed Steel (HSS) end mills of 1/16" (1.5875 mm) diameter, shank length 3/16" (0.1875 mm), and length of cut 0.1875" (4.7625 mm) were used.

The range of hole depth steps used in the experiments was from 0.0005" (0.0127 mm) to 0.0404" (1.026 mm). A centering microscope of 25X magnification and cross wire division, each of 0.001 inch, was used to enable the drilled hole center to coincide with the strain-gage circle center within the range of 0.004D, where D is 0.202 in.

The strain-gage rosette was mounted on the surface of the machined workpiece by pointing the strain-gage 1 in the direction of cutting speed and strain-gage 3 in the direction of the feed, as shown in Figure 3.4. Also, the radial distance from the center of the work piece was maintained constant for all the tests to confirm consistency.

The three strain-gages on the rosette were connected to a digital strain indicator unit with a switch and balance unit. Each strain-gage recorded a strain value when a hole

was drilled into the surface of the material. All the readings were used for residual stress calculations, the procedure of which is mentioned below.

### 3.4.2 Residual Stress Calculation

The residual stresses were calculated from the recorded strains as per ASTM standards E837 [10]. There are several mathematical methods developed for calculating nonuniform residual stresses in thick materials by considering the evolution of the strains measured from the incremental hole-drilling measurements [13]. These strain measurements are made on the surface of the specimen, which yields the greatest sensitivity to the residual stresses close to surface. Sensitivity to the interior stresses completely disappears at depths beyond about half the mean diameter of the hole-drilling rosette.

H-Drill mathematical software [14,15] was used to calculate residual stresses. Depending on the variation in the residual stress sensitivity to experimental errors and high spatial resolution, there are three stress calculation methods used by H-Drill:

Uniform stress method: This method is specified in ASTM 837. There is no spatial resolution, since the residual stresses are considered uniform with the depth from the specimen surface. This method is the least sensitive to the effects of experimental errors.

Power series method: This method assumes that the residual stresses vary linearly with depth from the specimen surface. Compared to the uniform stress method, this method is more sensitive to the effects of experimental errors. This method is a good

option when it is sure that the variation in the measured residual stresses is smooth with respect to depth.

Integral method: Spatial resolution is the highest for the integral method. In this method, during the hole-drilling measurements, residual stresses are evaluated separately within each increment of depth.

The integral method was chosen as the most appropriate calculation method among the three methods based on better strain misfit plots, and the expected trend in stress plots. It is assumed that in the Integral method, the stress within each hole-depth increment is uniform. Also, the software estimates the residual stresses calculated at the midpoints between two input hole-depth steps.

It is fundamentally known that failure occurs along the principal stresses plane; hence, maximum principal stresses are used to analyze the residual stress effects in this thesis [1,16].

## 3.5 References

1. Almen, J.O. and Black, P.H., 1963, Residual stresses and fatigue in metals, McGraw-Hill Book Company, Inc., USA.
2. Armarego, E. J. A. and Samaranayake, P. (1999) 'Performance prediction models for turning with rounded corner plane faced lathe tools. I. Theoretical development', *Machining Science and Technology*, Vol. 3(2), pp. 143-172.
3. Balaji, A.K. and I.S. Jawahir, (2001) 'Variable tool-chip interfacial friction in 2-D and 3-D machining operations', *Int. J. Forming Processes*, Vol. 4(1-2), pp. 111-123.
4. Bulletin 309E, "Student manual for strain gage technology," Vishay Measurements Group, Inc., <[www.vishay.com](http://www.vishay.com)>
5. Classification and Designation of Carbon and Low-Alloy Steels, Properties and Selection: Irons, Steels, and High-Performance Alloys, Vol 1, *ASM Handbook*, ASM International, 1990, p 140–194.
6. 'Determining Residual Stresses by the Hole-Drilling Strain-Gage Method' (1999) *Standard Test Method E837-99*. American Society for Testing and Materials.
7. Ghatikar, V. (2010) 'Design of Minimal Quantity Cutting Fluid dispensing system for sustainable machining'. *MS Thesis*, University of Utah.
8. 'Industrial ZYGO NewView 5000™ Precise, Rapid, Noncontact 3D Surface Profiling Corporation's', (2001), [www.zygo.com](http://www.zygo.com).
9. Jayal, A. D. (2006) 'An experimental investigation of the effects of cutting fluid application on machining performance', Phd dissertation, University of Utah.
10. Mathar, J. "Determination of Initial Stresses by Measuring the Deformation Around Drilled Holes." *Transactions of the American Society of Mechanical Engineers*, Vol.56, No.4, pp.249-254, 1934.
11. Measurements Group Tech Note TN-503, "Measurement of Residual Stresses by the Hole-Drilling Strain-Gage Method," Vishay Measurements Group, Inc., [www.vishay.com](http://www.vishay.com).
12. Redetzky, M., Balaji, A.K., Jawahir, I.S. (1999) 'Predictive modeling of cutting

Field Code Changed

Formatted: Font: Not Italic

Formatted: Font: Not Italic

Formatted: Font: Not Italic

Formatted: Font: Not Italic

13. forces and chip flow in machining with nose radius tools', Proc. 2nd CIRP Int. Workshop on Modeling of Machining Operations, Nantes, France, pp.160-180
14. Rendler, N.J., and Vigness, I., 1966, "Hole-drilling strain-gage method of measuring residual stresses," Experimental Mechanics, Vol. 6(12), pp. 577-586
15. Schajer, G. S., 2001, "Hole Drilling Residual Stress Calculation Program", Version 2.20
16. Schajer, G. S. and Steinzig, M., 2005, "Full-field calculation of hole drilling residual stresses from electronic speckle pattern interferometry data," Experimental Mechanics, Vol. 45(6), pp. 526-532
17. Shaw, M.C., 1984, Metal Cutting Principles, Oxford University Press, USA.

|

## **CHAPTER 4**

### **RESULTS AND DISCUSSION**

This chapter emphasizes the results of a study on the effects of targeted application of different cutting fluid combinations on various machining performance parameters such as machining forces, predicted chip flow angle, tool-chip contact area, chip morphology, surface roughness, and residual stresses in machining of 1045 plain carbon steel under certain fixed cutting conditions. Cylindrical bars of AISI 1045 steel were selected enabling the direct comparison of results with other work on similar materials in the literature. A facing operation that is closely similar to orthogonal machining (plain strain) was chosen such that a flat surface that could be appropriately analyzed was the targeted outcome. It was made sure that the cutting region is properly exposed to the cutting fluids disposed from two different nozzles, one being the coolant and the other lubricant from their respective sources.

AISI 1045 steel is a continuous chip forming material and this enabled the study of chip formation at different cutting fluid combinations application [9]. The experimental set up and the cutting fluid flow rate proportion combinations are mentioned in the previous chapter (Table 3.2) and in Table 4.1. The flow through the nozzles was regulated such that the total amount of fluid from both the nozzles together was 60ml/hr under a pressurized air stream at ~0.6 MPa.



Table 4.1 Cutting fluid combinations

100% = 60 ml/hr, 75% = 45 ml/hr, 50% = 30 ml/hr, 25% = 15 ml/hr

Experiment	% of Coolant (C)	% of Lubricant (L)
1 (Dry)	0	0
2 (rake face)	100	0
3 (rake face)	75	25
4 (rake face)	50	50
5 (rake face)	25	75
6 (rake face)	0	100
7 (flank face)	100	0

It was ensured that the cutting fluid nozzles were directed at about 2 mm from the corresponding cutting tool face (rake or flank) to ensure consistent cooling and/or lubrication and uniformity in comparison of results.

#### 4.1 Machining Forces

Cutting forces were measured using a Kistler® three-component dynamometer (9121) interfaced with Kistler® charge amplifiers (5010) connected to a National Instruments Labview™-based data acquisition system with a PCI 6703 DAQ card.

Figure 4.1 shows the feed, radial (thrust), and main cutting forces plotted against each cutting fluid combination/application. The thrust force in all cases remained similar, which implies that the experiment resembles orthogonal machining (wherein there is no 3<sup>rd</sup> or radial component effect). The feed force and cutting force followed similar trends

explaining the significance of the introduction of cutting fluid. The force values lowered with the addition of lubricant and/or coolant on the rake face as compared to dry environment and 100 % coolant on the flank face. The dispensing of both coolant and lubricant on the rake face helped in the reduction of high local temperatures as well as friction, which resulted in lower force values. The targeted application of cutting fluid combinations did not show any significant effect on the force variation since air and coolant (water) also act as lubricants.

On the other hand, the feed and cutting forces obtained for 100% coolant on the flank face without any lubricant were slightly higher when compared to the forces in dry machining and other cases. This can be explained by the fact that the coolant had not reached the main cutting edge (rake face) as opposed to other cases and the flank face application has no effect in reducing tool-chip interfacial friction or tool temperature at the rake face (both factors which can reduce the force components in a machining operation). Similarly, in dry machining, since no fluid was used, slightly higher force components were recorded.

#### 4.2 Prediction of Chip Flow Angle

An algorithm from a comprehensive predictive model for cutting forces and chip flow in machining with nose radius tools developed at University of Kentucky [1,15] was used to predict the chip flow angle for the cutting conditions tested in this thesis and plotted in Figure 4.2. The chip flow angle was lower for the cases with higher cutting forces and vice versa and thus the strong correlation of chip flow direction to the magnitude of the cutting force components (main, feed, and radial) is verified [4,7,15].

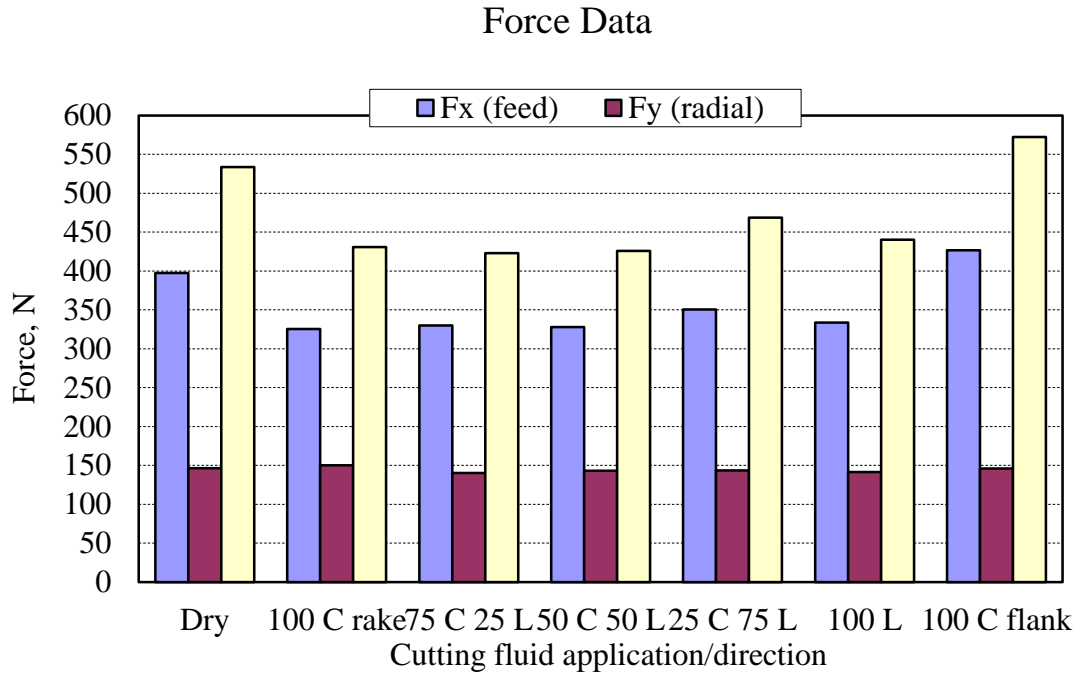


Figure. 4.1 Force data: Effect of cutting fluid combination application on cutting forces during facing operation with flat-faced carbide tool at 0.1 mm/rev feed rate, cutting speed of 225 m/s, and a depth of cut of 1.2 mm

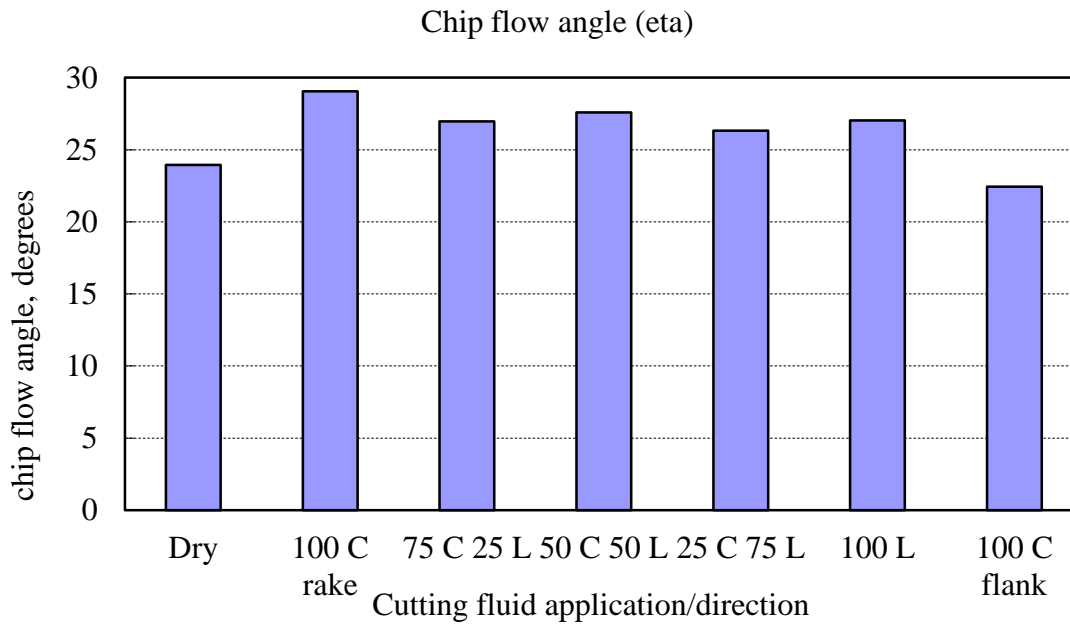


Figure. 4.2 Chip flow angle: Predicted chip flow angle at different cutting fluid application combinations/directions

Dry and 100% coolant on Flank conditions produced the smallest angles of chip flow, indicating relatively higher frictional conditions at the tool rake face due to the lack of coolant or lubricant application.

#### 4.3 Tool-Chip Contact and Chip Morphology

Scanning Electron Microscope (SEM) imaging analysis was conducted on the rake face of the flat-faced carbide tool (after machining) to study the tool-chip contact area traces for each case of cutting fluid application. The interaction between the tool and chip is the primary phenomenon controlling the tribological performance in machining. It is across the tool-chip interface that the forces necessary to form the chip are transmitted.

The parameters that influence the nature of tool-chip contact in machining are cutting tool stresses, thermal conductivity, and friction between cutting tool and chip [3,4]. Tool-chip contact (Figure 4.3) did not show any significant difference corresponding to different cutting fluid combinations applied on the tool rake face. However, when there was no coolant and/or lubricant application on the tool rake face (Dry and 100% Coolant on flank), there was significantly larger contact at the tool-chip interface (Figure 4.4), which is indicative of higher tool-chip interfacial friction and intense tribological conditions.

The chips generated (Figure 4.5) during dry machining and 100% coolant on the flank face were up-curved, long, continuous ribbon shaped, while for all other cases, the chips were side-curved, cork-screw helical shaped (diameter of the curl varied from 9 to 12 mm), followed by discontinuous small chips, which correspond to the cutting force variation.

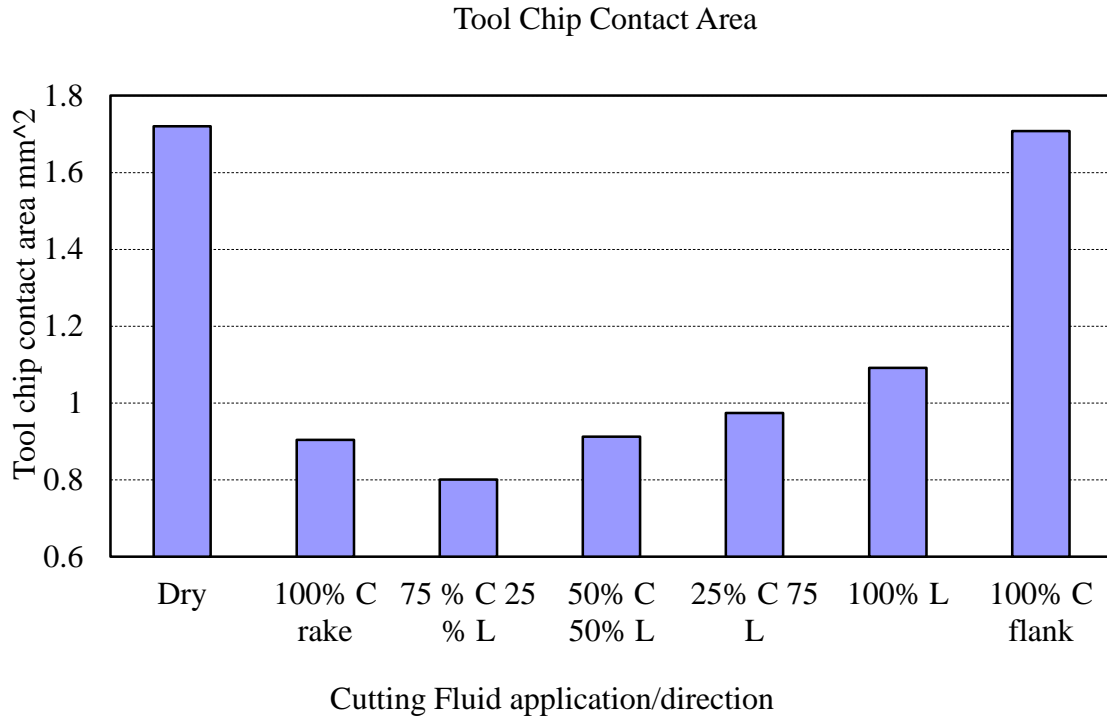


Figure. 4.3 Tool-chip contact area (mm<sup>2</sup>) at different cutting fluid application combinations/direction

The nonlinear variations in 3-D machining due to the nose radius and the cutting edge angle caused sideward flow on the tool rake face [4].

Since the lubricant and coolant were directed onto the rake face, the force of the fluid stream helped in breaking the chips to form discontinuous side-curved, helical shaped pieces.

The explanation is directly related to the trend followed by the cutting force values for the respective experiments. The scientific reasoning for the chip formation is elaborated in the residual stress discussion.

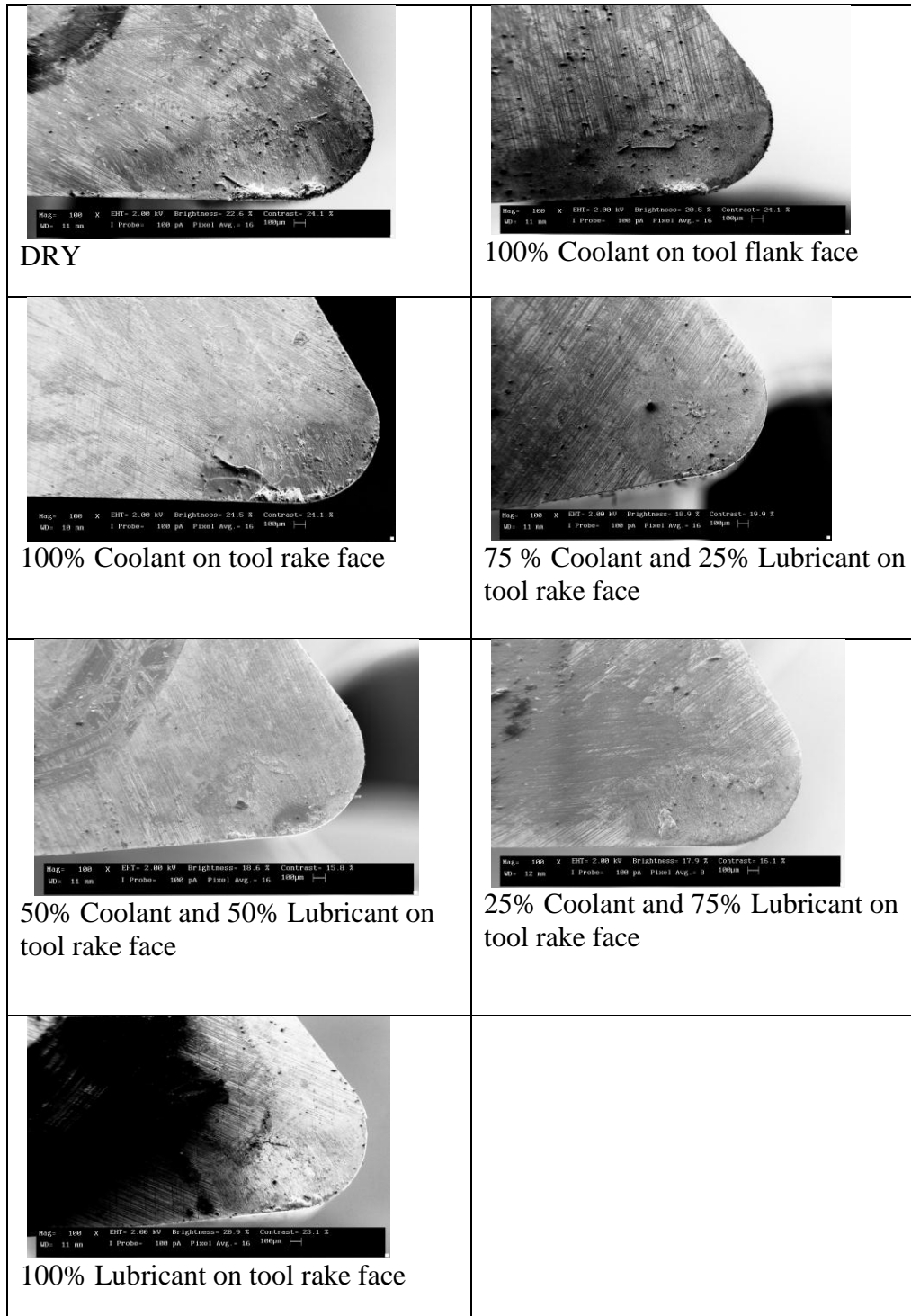


Figure. 4.4 Tool chip interfacial contact, SEM images of flat faced carbide tool (nose radius 0.8 mm, rake angle  $-7^\circ$  and included angle  $60^\circ$ )

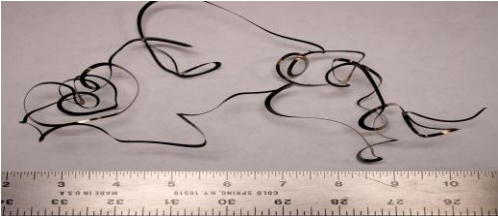
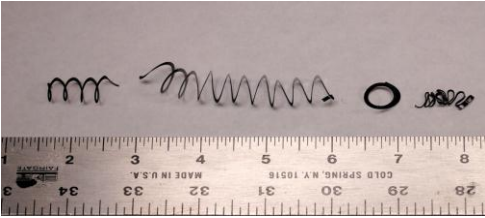
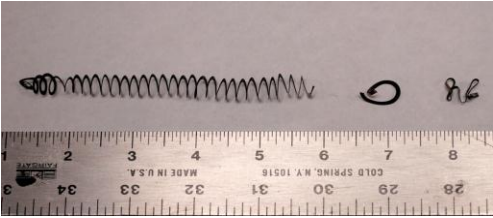
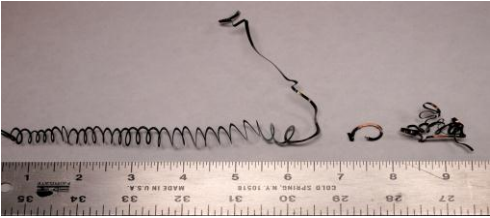
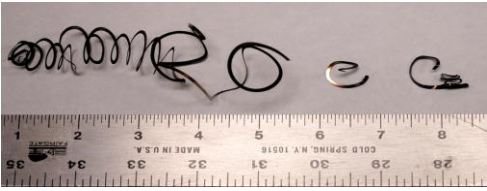
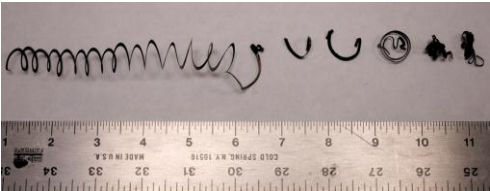

 <p>DRY</p>	 <p>100% Coolant on tool rake face</p>
 <p>75 % Coolant and 25% Lubricant on tool rake face</p>	 <p>50% Coolant and 50% Lubricant on tool rake face</p>
 <p>75 % Coolant and 25% Lubricant on tool rake face</p>	 <p>100% Lubricant on tool rake face</p>
 <p>100% Coolant on tool flank face</p>	

Figure 4.5 Chip forms obtained at different cutting fluid combinations

#### 4.4 Surface Roughness

The surface roughness values of the machined work pieces were measured using a Zygo<sup>®</sup> NewView 5000 series optical interferometry-based surface profilometer. A cutoff (roughness sampling length) value of 0.8 mm was used while estimating the average roughness profile ( $R_a$ ) as recommended [11].

The average roughness ( $R_a$ ) values obtained at different locations on the surface of the machined work piece were used to analyze the effects of different cutting fluid combinations on surface roughness.

It was observed (Figure 4.6) that dry machining produced the highest surface roughness ( $R_a$ ) values. Due to the combined effects of friction and temperature induced at the cutting zone, the chips tend to create a strong adhesive tendency at the tool-chip interface (as confirmed by the larger tool-chip contact area). The huge cluster of long continuous chips at the work piece-tool interface could have added to the larger roughness value in dry machining. The chips produced when using 100% coolant on the flank face were not as long as in dry machining and the coolant jet helped in throwing away the cluster from the machined surface, which explains the reason for the lowest average surface roughness. Furthermore, it can be seen that directly applying a mist of 100% coolant in the flank (which is the tool surface most close to the machined surface) has an immediate direct impact in smoothening the machined surface. The addition of cutting fluid dropped the  $R_a$  values of all the other cases to within 1.5 to 2  $\mu\text{m}$  of the surface roughness of dry machining that verifies the functionality of cutting fluid (cooling and/or lubrication).



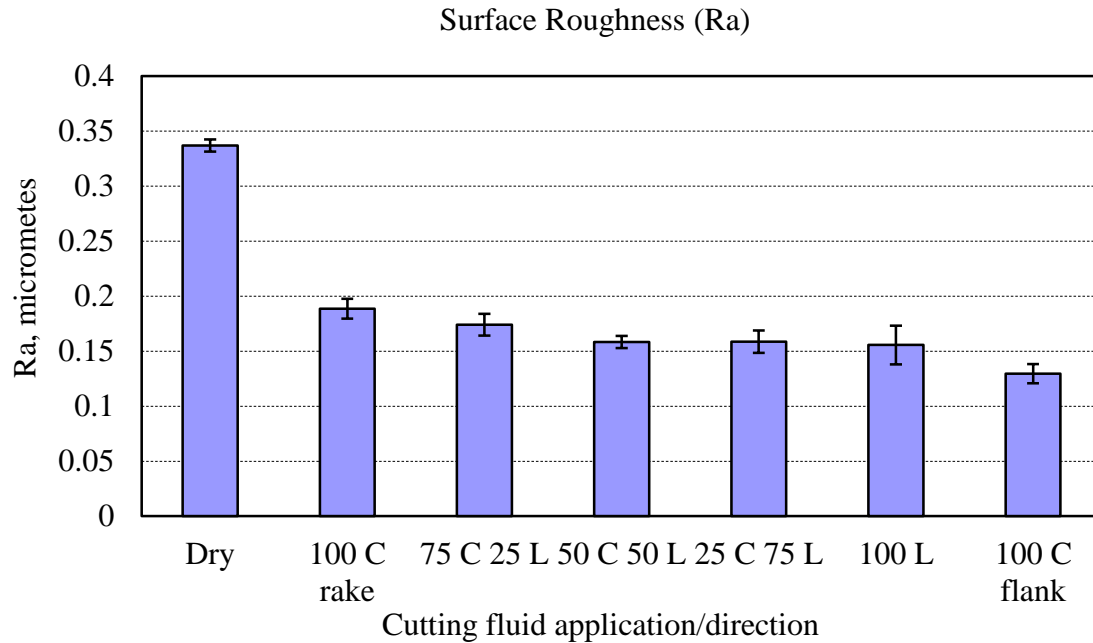


Figure. 4.6 Surface roughness: Average surface roughness ( $R_a$ ) for each cutting fluid application combinations/direction.

#### 4.5 Residual Stresses

Postmachining measurement of residual stresses on the machined work pieces using incremental hole-drilling strain-gage method disclosed some interesting results that lead to a new insight on the influence of the direction and composition of the cutting fluid on machined surface integrity. As shown in this section, the importance of directing the cutting fluid, especially minimal coolant with pressurized air stream onto the flank face of the tool, is strongly amplified.

Residual stresses measured in the subsurface of the machined work piece are caused due to the thermal effect of the temperature distribution encountered in metal cutting and the mechanical effect of the ploughing force at the cutting tool edge. The thin ploughed depth, which is a small fraction of uncut chip thickness, is the controlling factor for residual stress profiles in the machined subsurface. This threshold depth experiences

high transient stresses, large strains, and strain-rates at high temperatures with severe gradients. Friction influences the magnitude of the surface residual stress. A “hook” shaped residual stress profile generated while machining with a fresh tool is characterized by surface compressive residual stress and maximum compressive residual stress in the subsurface [8]. However, small changes in cutting conditions (or cutting fluid application, as shown in this thesis) can drastically change the nature and magnitude of such stress profiles.

Figure 4.7 through Figure 4.12 present the principal residual stresses (MPa) plotted against their respective hole depths (mm) in which each cutting fluid combination application case is compared to the dry machining condition. Maximum principal residual stresses were considered for all cases to ensure uniformity and consistency, as the magnitude of residual stress did not vary much between maximum and minimum principal residual stresses. Previous studies [6,8,10] indicate that stresses are concentrated near the surface of ductile materials such as carbon steels and thus result in high tensile residual stresses in the metal surface by the action of a cutting tool even when light cuts (low feed rates) are performed.

The induced stresses are also closely related to the hardening properties of the material. The possible phenomena responsible for hardening are plastic work (work hardening) and quenching (tempering). In the present work, plastic work and quenching play a major role in affecting the hardening methods and hence the residual stresses.

Figure 4.7 compares the principal residual stresses obtained for dry machining against the 100% lubricant on the rake face condition.

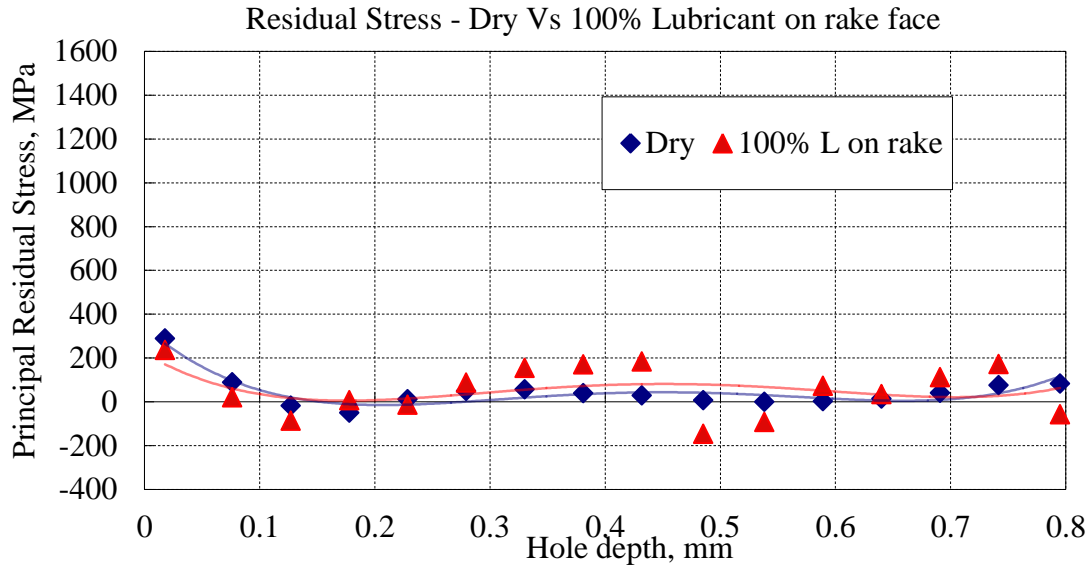


Figure 4.7 Residual stress plot-Dry Vs 100% lubricant on the rake face

It is observed that the two cases follow a similar trend except that, the near surface residual stress lowered marginally with the introduction of lubricant onto the rake face.

Due to adhesion, there was sticking and sliding of the flowing chip on the tool rake face, there is more scope for friction to be induced, which in turn results in plastic deformation, adhering of chip material to the tool rake face, and possibly high temperatures. The high-pressure air and oil jet helped in reducing friction between the work piece-tool interface and hence reduced the total tool-chip interfacial temperature caused by friction [2,14]. This reduction in friction also reduced the temperature gradient. Since an uncoated tool was used for the tests, some of the heat was conducted into the tool, which resulted in lower tensile residual stresses [12]. Also 100% lubrication on the rake face case produced discontinuous side-curved helical chips. Directing the lubricant onto the rake face served its purpose of controlling temperatures induced due to friction.

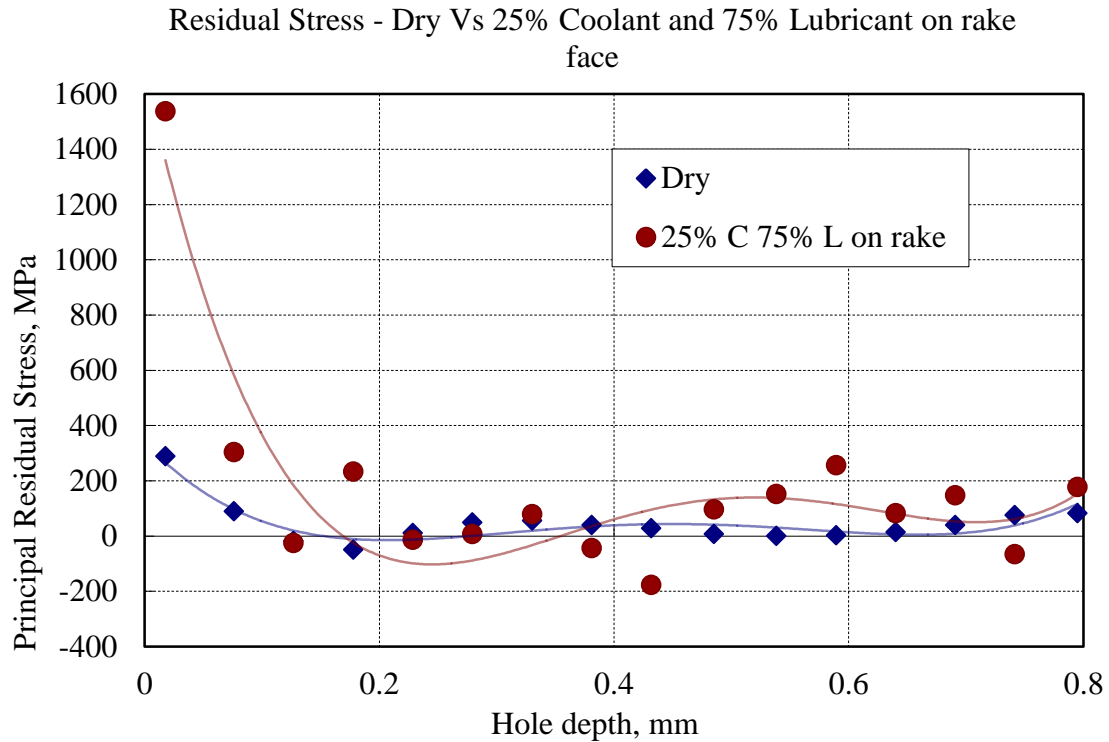


Figure 4.8 Residual stress plot-Dry Vs 25% coolant and 75% lubricant on the rake face

The residual stress plot when using proportions of coolant and lubricant at 25% and 75%, respectively, onto the rake face of the tool are shown in Figure 4.8.

The residual stresses followed the same trend as that in dry machining after a hole depth of  $\sim 0.125$  mm, but the near surface residual stress due to 25% coolant and 75% lubricant jumped up to 1537 MPa. This case exhibited the highest surface residual stress among all other cases. This is very interesting because it appears that just adding a small amount (25%) of coolant to the mixture drastically changes the surface integrity of the machined surface. Somehow, this small addition of coolant (and proportional decrease of lubricant) was strong enough to significantly change the surface residual stress. However, the internal stress profile does not change much.

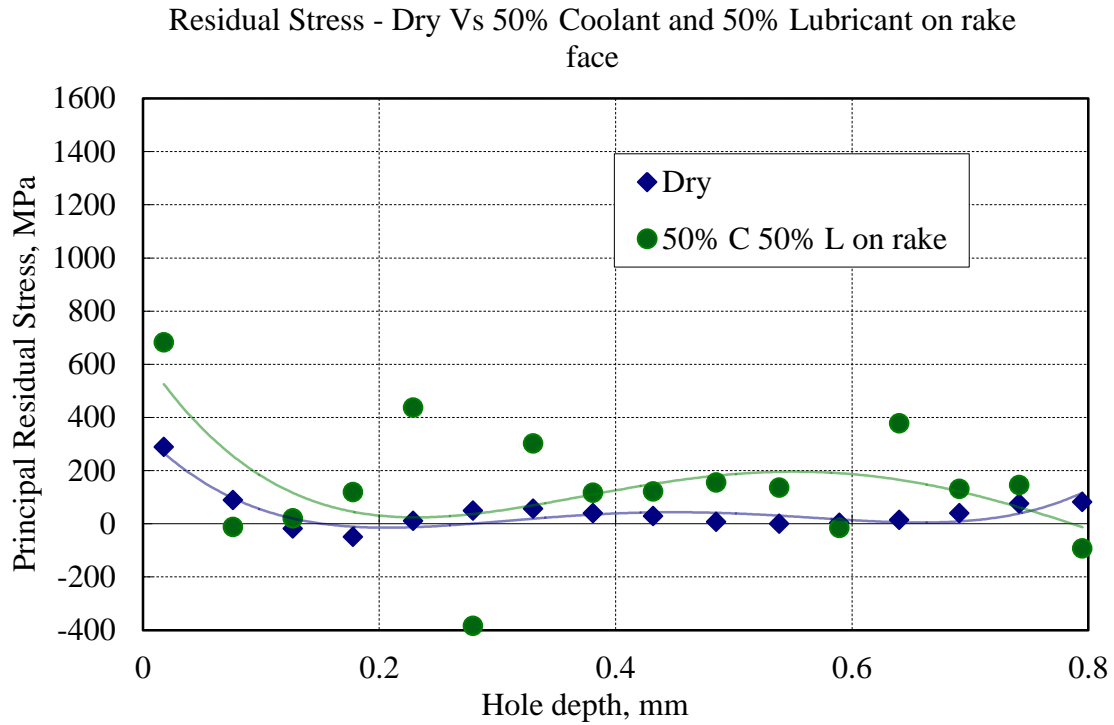


Figure 4.9 Residual stress plot-Dry Vs 50% coolant 50% lubricant on the rake face

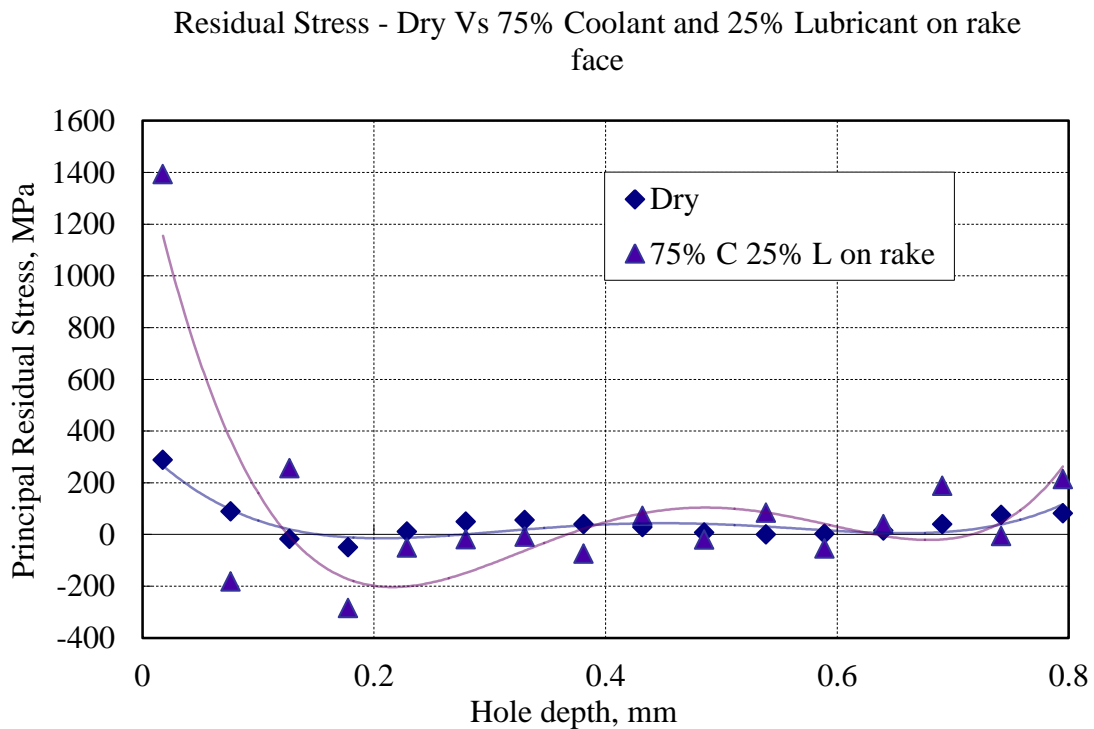


Figure 4.10 Residual stress plot-Dry Vs 75% coolant and 25% lubricant on the rake face

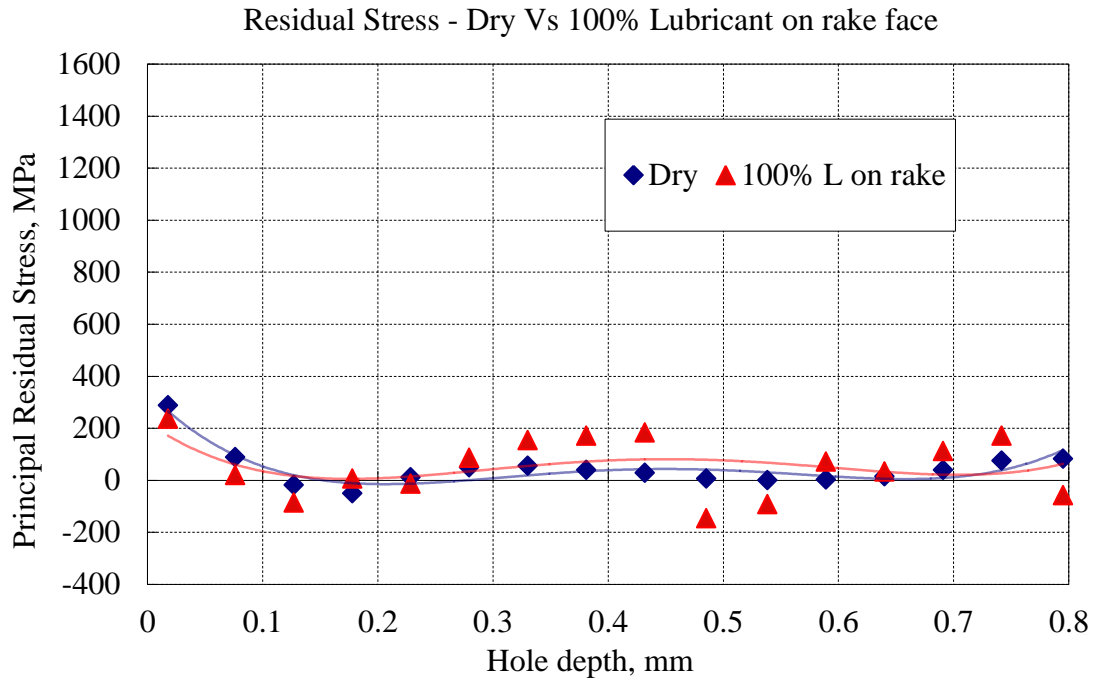


Figure 4.11 Residual stress plot-Dry Vs 100% coolant on the rake face

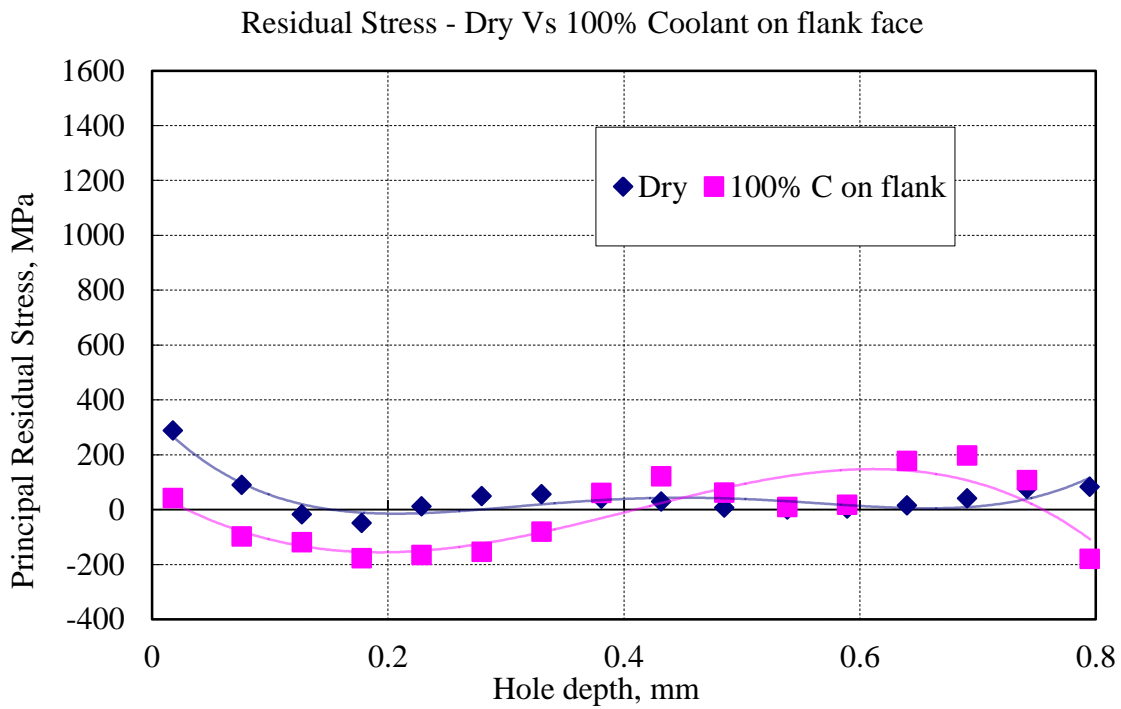


Figure 4.12: Residual stress plot-Dry Vs 100% coolant on the tool flank face

The introduction of coolant along with the lubricant in a compressed air jet increased the thermal gradient and plastic strain at the cutting zone, leading to high surface residual stress.

Figures 4.9 and 4.10 show the residual stress plots for cutting fluid combinations of 50% coolant and 50% lubrication on the rake face and 75% coolant and 25% lubricant on the rake face. They exhibited similar trends as 25% coolant and 75% lubricant, with very high near surface residual stress when compared to dry machining.

50% coolant and 50% lubricant on the rake face showed slightly lower surface residual stress (682.014 Mpa) when compared to other coolant and lubricant combination cases (Figure 4.8 and Figure 4.10), the reason for which is not yet clear.

The deposition of coolant on the rake face of the tool along with the lubricant led to quenching action on the tool rake face, which lowered the thermal softening in the work zone, simultaneously increasing plastic work and thus resulting in high tensile stress. 100% coolant on the rake face, as shown in Figure 4.11, showed similar behavior.

The experiment with 100% coolant on the rake face induced considerably high surface residual stress but it was evident that it was less than other coolant and/or lubricant combination cases, which emphasize that the coolant under compressed air jet can act as a lubricant in itself.

In contrast, the experiment with 100% coolant on the flank face (Figure 4.12) showed the lowest near surface residual stress when compared to dry machining and all other cases. The mechanism involved here can be understood by the following explanation. While cutting, the flank face rubs along the machined surface and tends to induce high thermal gradient due to friction and plastic deformation. This emphasizes

that coolant on the flank face quenches the work piece - tool interface and thus results in relatively compressive surface residual stresses. Further, the plastic strain at the ploughing layer is reduced along with the subsurface temperature. The coolant was not directed to the chip underside, thus not breaking the chips, and the flat-faced tool allowed the formation of long continuous chips. This led to more sticking and sliding on the tool rake face and resulted in a slightly higher tool-chip contact area as compared to other cases. However, directional application of the coolant on the flank specifically improved the surface integrity of the machined surface, although it had negative impact on tribological performance at the tool-chip interface.

This is an important finding in this thesis: we cannot have a single solution that automatically provided enhanced tribological performance (reduced tool-wear, reduced frictional contact at rake face) and enhanced surface integrity (high compressive residual stresses). Targeted, localized, and minimized application of the ideal and necessary medium has the potential to produce better results.

It was observed that the obvious characteristic of coolant (water) to perform quenching action can be both advantageous as well as detrimental. When the coolant is directed onto the rake face, high surface tensile residual stresses were induced, while the same quenching action on the flank resulted in inducing compressive surface residual stresses.

Figure 4.13 shows the peak residual stresses of each cutting fluid application combination/direction. Clearly, it is evident that with the application of coolant on the flank face, compressive residual stresses were induced. Quenching might have occurred on the flank face.



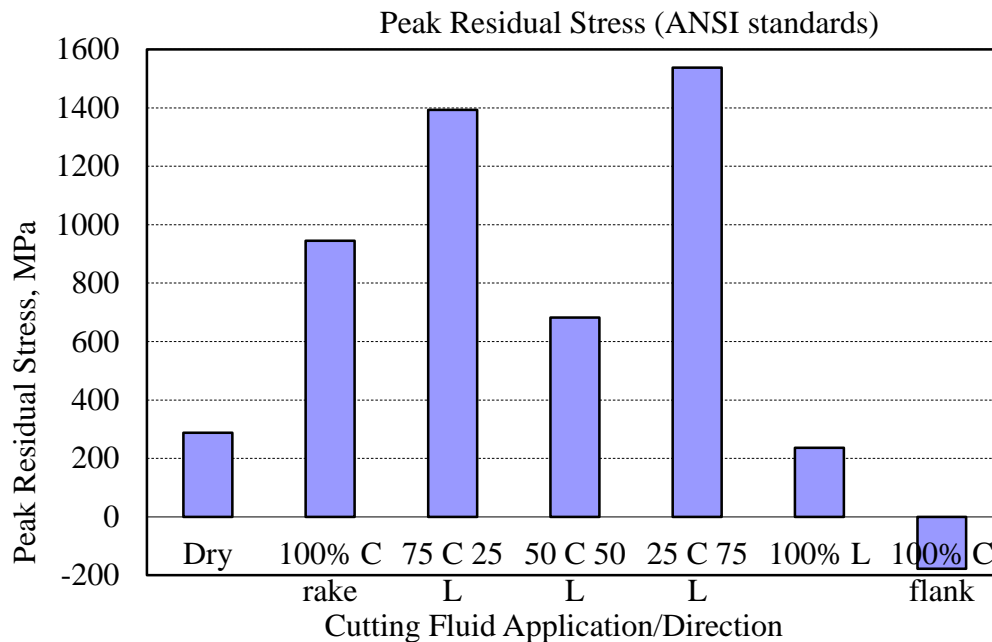


Fig. 4.13: Peak residual stresses at different cutting fluid application combinations

Researchers found that residual austenite is detected on the friction face of the chip (tool-chip interface) and on the machined surface of the carbon steels. This austenite occurrence is associated with high temperatures in conjunction with shearing and high hydrostatic pressure. This phenomenon can be explained by the fact that “due to high pressure/shear the pearlite to austenite transformation temperature is reduced and causes austenite formation.” Due to quenching [16] at the flank face, austenite might have been transformed to martensite. This in turn led to compressive residual stress formation.

This implies that directing the coolant on the flank face could induce compressive residual stresses in the work piece. Figure 4.13 shows that 100% coolant on the flank face produced compressive residual stresses. It is thus understood that directing the coolant under pressurized air onto the flank face allows the surface of the work piece to produce compressive stresses, which is desirable for a better machined surface integrity.

From the experimental evidence, it can be inferred that the residual stress pattern can be correlated to the direction and proportion of the cutting fluid applied. It can be emphasized that delivering coolant on the flank face and lubricant onto the rake face can induce lower surface and subsurface residual stresses (compressive stresses) and better surface finish for the given material, tool, and cutting conditions when compared to dry machining.

#### 4.6 Discussion

In a nutshell, the effect of targeted cutting fluid combinations application on the triobological aspects is limited, under the cutting conditions employed in this thesis. Dispensing the coolant on the tool flank face recorded slightly higher main cutting force, indicating the inability to alter frictional and thermal conditions in the cutting zone (rake face), since the influence of coolant on the tool-chip contact area was minimal. Consequently, the tool-chip contact area was marginally higher for coolant on the flank face (tool-chip contact area close to dry machining) when compared to other cutting fluid combinations application. The higher surface roughness value for dry machining indicates that the cutting fluid application significantly influenced the surface roughness of the machined surfaces. Chip flow angle and chip formation showed similar trends with the application of cutting fluid on the tool face.

The principal residual stress obtained for each cutting fluid combination application showed significant variations. The application of coolant on the tool flank face showed some interesting results. As fundamentally implied, the friction induced on the main cutting edge (tool rake face) is influenced by the lubricating action of oil, while the high temperatures transpired at the secondary cutting edge (tool flank face) are

controlled by the application of coolant [9, 10]. This fact has been clearly identified in this work from the peak residual stresses induced near the surface of the machined work piece. Evidently, the application of coolant on the tool flank face and lubricant on the tool rake face induced compressive residual stresses and relatively low tensile residual stresses, respectively.

A detailed summary on the study of the effects of targeted cutting fluid combinations application is presented in Chapter 5, along with some recommendations for extended future research.

## 4.7 References

1. Armarego, E. J. A. and Samaranayake, P. (1999) 'Performance prediction models for turning with rounded corner plane faced lathe tools. I. Theoretical development', *Machining Science and Technology*, Vol. 3(2), pp. 143-172.
2. Attanasio, A., Ceretti, E., Gelfi, M. and Giardini, C. (2009) 'Experimental evaluation of lubricant influence on residual stress in turning operations', *Int. J. Machining and Machinability of Materials*, Vol. 6 (1/2), pp. 106-119.
3. Balaji, A.K., G. Sreeram, I.S. Jawahir and E. Lenz, (1999) 'The effects of cutting tool thermal conductivity on tool-chip contact length and cyclic chip formation in machining with grooved tools', *Annals of the CIRP*, Vol. 48(1), pp. 33-38.
4. Balaji, A.K. and I.S. Jawahir, (2001) 'Variable tool-chip interfacial friction in 2-D and 3-D machining operations', *Int. J. Forming Processes*, Vol. 4(1-2), pp. 111-123.
5. Balaji, A.K. and Jawahir, I. S. (1999) 'Variable Tool-Chip Contact and Chip Morphology in Machining with Grooved Cutting Tools: A Tribological Perspective'.
6. Field, M., Kahles, J.F. (1971) 'Review of surface integrity of machined components', *Annals of the CIRP*, Vol. 20(2), pp.153-162.
7. Ganapathy, B.K., Jawahir, I.S. (1998) 'Modeling the chip-work contact force for chip breaking in orthogonal machining with a flat-faced tool', *ASME Journal of Manufacturing Sc. & Engg.*, Vol. 120(1), pp.49-56.
8. Guo, Y.B., Li, W. and Jawahir, I.S. (2009) 'Surface integrity characterization and prediction in machining of hardened and difficult-to-machine alloys: A state-of-art research review and analysis', *Machining Science and Technology*, Vol. 13, pp.437-470.
9. Jayal, A. D. (2006) 'An experimental investigation of the effects of cutting fluid application on machining performance', *Phd dissertation, University of Utah*.
10. Liu, C. R. and Barash, M. M. (1976) 'The Mechanical State of the Sublayer of a Surface Generated by Chip-Removal Process', *Transactions of the ASME, Journal of Engineering for Industry*, pp.1192-1201.
11. Machinery's Handbook – Surface Texture.
12. Outeiro, J. C. and Dias, A. M. (2006) 'Influence of Work Material Properties on Residual Stresses and Work Hardening Induced by Machining', *Materials Science Forum*, Vol. 524-525, pp. 575-580.

13. Oxley, P. L. B. (1989) 'The mechanics of machining: An analytical approach to assessing machinability', Ellis Horwood Ltd., Chichester, UK.
14. Rahman, M. M., Khan, M. M. A. and Dhar, N. R. (2009) 'An experimental investigation into the effect of minimum quantity lubricant on cutting temperature for machinability of AISI 9310 steel alloy', *European Journal of Scientific Research*, Vol. 29(4), pp. 502-508.
15. Redetzky, M., Balaji, A.K., Jawahir, I.S. (1999) 'Predictive modeling of cutting forces and chip flow in machining with nose radius tools', *Proc. 2nd CIRP Int. Workshop on Modeling of Machining Operations*, Nantes, France, pp.160-180.
16. Changeux, B. and Lebrun, J.-L. (2001) 'Microstructural modifications and material response in machining of steels', *Journal of Physics France*, Vol. 11, pp. 213-220.

## CHAPTER 5

### SUMMARY AND SCOPE FOR FUTURE WORK

An experimental study was conducted to investigate triobological effects and surface integrity by facing cylindrical bars of 1045 steel using flat-faced uncoated carbide tools, with 0.1 mm/rev feed rate, 1.2 mm depth of cut, and 225 m/min cutting speed. Different minimal quantity combinations of coolant and/or lubricant directed on the rake/flank face were considered along with dry cutting. During the process, a Minimal Quantity Cutting Fluid dispensing system was modeled and used for the tests, which helped in dispensing the regulated amounts of cutting fluid via an electronic signal from a LabView program.

The results demonstrated the importance of directing the right fluid onto the corresponding cutting tool face. The cases with 100% lubricant on the rake face and 100% coolant on the flank face gave better surface residual stresses than dry and all other cases. These two cases had better surface roughness as opposed to all other cases. The experiment with dry environment served as a reference for all other cases. There was no significant difference or advantage that could be inferred from the coolant and lubricant combinations directed onto the rake face.

The scope of this thesis is of necessity limited. It deals with low strength carbon steel with a single-point cutting tool, fixed cutting conditions, and varying

cutting fluid combination application targeted on different tool faces. This hints that future work can be undertaken on the effect of various combinations of work materials, cutting fluids, and cutting conditions. Microstructures could be studied to determine the martensitic formation in detail. Further, the investigations can be used to correlate the induced stresses to cutting forces, which could contribute to the general knowledge of the mechanism of cutting and would also give designers and manufacturers an in-depth understanding of machining performance for them to choose better and safer materials and methods.